Naphthalene Diimide For Selective Telomeric G-Quadruplexes: Synthesis And Characterization

Zahra Modjtahedi

Submitted to the
Institute of Graduate Studies and Research
in partial fulfillment of the requirement for the Degree of

Master of Science
in
Chemistry

Eastern Mediterranean University
February 2015
Gazimağusa, North Cyprus

Approval of the Institute of Graduate Studies and Research

_____
Prof. Dr. Serhan Çiftçioğlu
Acting Director

I certify that this thesis satisfies the requirements as a thesis for the degree of Master of Science in Chemistry.

_____
Prof. Dr. Mustafa Halilsoy
Chair, Department of Chemistry

We certify that we have read this thesis and that in our opinion it is fully adequate in scope and quality as a thesis for the degree of Master of Science in Chemistry.

_____
Prof. Dr. Huriye İcil
Supervisor

Examining Committee
_____

1. Prof. Dr. Huriye İcil   _____

2. Asst. Prof. Dr. Jagadeesh B. Bodapati   _____

3. Asst. Prof. Dr. Hürmüs Refiker   _____

ABSTRACT

Nowadays, as a result of developing new technologies, the applications of organic substances utilized in various fields are growing interest. The naphthalene diimides, due to their excellent electrochemical, thermal and photophysical properties as well as their excellent light emitting potentials have been intensively investigated as electronic materials in photonic applications. In addition, naphthalene diimides are used as potential ligands in biological applications, especially in DNA binding.

In this research, N,N'-bis(2-(4-hydroxyphenyl)ethyl)-1,4,5,8-naphthalenediimide (HE-NDI) has been synthesized successfully. The structure of product was characterized and investigated by optical and photophysical properties using FT-IR, UV-vis and emission spectroscopic techniques.

The HE-NDI has shown high molar absorptivity and fluorescence quantum yield. The results have pointed that the HE-NDI is a potential candidate for photonic application and DNA binding.

Keyword: Naphthalene diimide, Solar cell, Photovoltaic, DNA

ÖZ

Son zamanlarda, gelişen teknolojiyle birlikte birçok alanda organik maddelere ilgi artmaktadır. Naftalin diimidler sergiledikleri muhteşem elektokimyasal, termal, fotokimyasal ve ışık yayan özellikleri sayesinde fotonik uygulamalarda organik madde olarak yoğun bir şekilde incelenmektedirler. Bunun yanında, naftalin diimidler biyolojik uygulamalarda özellikle DNA bağlama konusunda potansiyel ligand olarak kullanılmaktadır.

Bu çalışmada, N,N'-bis(2-(4-hidroksifenil)etil)-1,4,5,8-naftalindiimid (HE-NDI) başarıyla sentezlenmiştir. Sentezlenen maddenin yapısı, optik ve fotofiziksel özellikleri FT-IR, UV-VİS ve emisyon teknikleriyle incelenmiştir.

HE-NDI yüksek molar absorplama ve floresan kuantum verimi göstermiştir. Sonuçlar HE-NDI'ın fotonik uygulamalar ve DNA bağlama için potansiyel bir aday olduğunu işaret etmektedir.

Anahtar Kelimeler: Naftalin diimide, Güneş pili, Fotovoltaik, DNA.

To My Family

ACKNOWLEDGMENT

First of all, I would like to express my special thanks to my supervisor Prof. Dr. Huriye İcil for giving me the great opportunity to study in her research group, and guiding and supporting me in all aspects of my master thesis. I will always remember her as a distinguished scientist. I am really lucky because I was her student.

Secondly, I would like to thank Dr. Duygu Uzun for her supports during my research.

I would like to thank all the researchers in the Organic Chemistry Group at the Eastern Mediterranean University for motivating and encouraging me with their endless love.

The last but not the least, I would like to thank my parents and my uncle for their support and encouragement.

TABLE OF CONTENTS

LIST OF TABLES

LIST OF FIGURES

LIST OF SCHEMES

LIST OF ABBREVIATIONS/SYMBOLS

Å	Armstrong
cm	Centimeter
^0C	Degrees Celcius
$\Delta\bar{\upsilon}_{1/2}$	Half-width of the Selected Absorption
ε_{max}	Maximum Extinction Coefficient
E_s	Singlet Energy
λ_{exc}	Excitation Wavelength
λ_{max}	Maximum Absorption Wavelength
τ_0	Theoretical Radiative Lifetime
τ_f	Fluorescence Lifetime
Φ_f	Fluorescence Quantum Yield
nm	Nanometer
$CHCl_3$	Chloroform
CHL	Chloroform
DMF	N,N'-dimethylformamide
DNA	Deoxyribonucleic acid
FT-IR	Fourier Transform Infrared Spectroscopy
HCl	Hydrochloric Acid
KBr	Potassium Bromide
k_f	Theoretical Fluorescence Rate Constant
M	Molar Concentration
MeOH	Methanol
MF	Microfiltration

RNA   Ribonucleic Acid

UV-vis   Ultraviolet Visible Absorption Spectroscopy

Chapter 1

INTRODUCTION

Rylene diimides are important dyes in different aspects of industry. They belong to a class of polycyclic aromatics with electron–transporting characteristics. Naphthalene derivatives (NDI) are π-functional conjugated members of the rylene family. They have excellent photochemical, electrochemical and thermal stabilities [1-2]. The properties of Naphthalene derivatives are improved by substitution from bay- and imide positions [3]. Therefore, they are used in Organic Field Effect Transistors (OFETS), n-type semiconductors, Organic light emitting diodes (OLEDS) and solar cell applications as electroactive materials. Naphthalene derivatives are also used in multicolor light harvesting and biological applications, such as DNA-binding [4-8]. The absorbance and fluorescence properties of naphthalene derivatives can be altered by substitution [9]. N-substitution (imide-substitution) of naphthalene derivatives controls the solubility, aggregation and intermolecular π-π stacking of molecules in the solid state. On the other hand, core (bay-) substitution of naphthalene derivatives affects optical and electronic properties as well as redox potentials [10]. In addition, their use in optoelectronic applications are limited since they do not absorb visible light [11]. The absorption range may increased by extending the conjugation of NDI from the core substitution with electron donor groups [12].

The solubility of NDI's in common organic solvents is low and limits their application in solution. Their solubilities can be improved by using long aliphatic substituents [13]. Brider et.al revealed that NDIs have the capability to bind deoxyribonucleic acid (DNA) [14]. The redox properties of NDI show strong ability to reduce and produce anionic radicals. With these properties, NDI's have interaction with biological molecules and are effective candidates for photodynamic cancer therapy [15]. G-quadruplex is a specific structure of DNA and NDI derivatives were used as G-quadruplex ligands with significant cellular toxicity [16]. The consequent delocalized electron system can thermally be stabilized with G-quadruplex and on the other hand, provides the stacking interactions [17]. On the other hand, the redox properties of NDI make them a good candidate for solar cell applications as electron acceptor material [18].

In this thesis, novel naphthalene diimide has been synthesized successfully (Scheme 1.1). The synthesized HE-NDI was characterized by FT-IR, UV-vis and emission techniques.
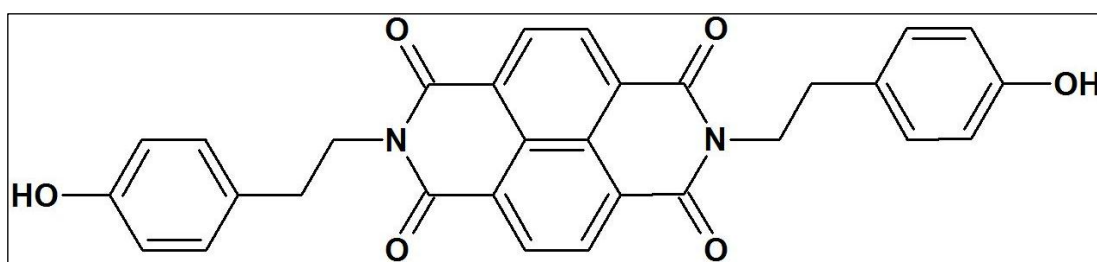
Scheme 1.1: Chemical Structure of N,N'- Bis(2-(4-hydroxyphenyl)ethyl)-1,4,5,8-naphthalenediimide (HE-NDI)

Chapter 2

THEORETICAL

2.1 Naphthalene Dyes: An Overview

Naphthalene dyes are well known as π-conjugated organic materials. They have high electrochemical, photochemical and thermal stability as well as molar absorptivities and light emitting abilities. These properties make them an important candidate for photonic applications and employed as an organic material in opto-electronic system. Moreover, they are extensively applied in organic electronic application, for example, organic light emitting diodes, field effect transistors and optical switches [19]. They are extensively applied as n-type materials due to a π-π^{*} interaction that supply delocalized electron system via electron affinities of imide groups. As a result, naphthalene dyes were used as semiconductors with n-type characteristics. Naphthalene derivatives have weak solubility that could be solved significantly by N-substitution. Due to the donor-acceptor pairs' capabilities of naphthalene derivatives, they are used in fluorescence resonance energy transfer (FRET) [20]. NDIs have some functional groups that give theme ability to bind with macromolecules. Carboxyl and amino groups are the most general of these groups. Naphthelene derivatives are also used in solar cells due to their absorption, emission and redox capability. In addition, they are used as intercalacting ligands in anticancer drugs. These small molecule ligands usually stabilize G-quadruplex DNA structure and even facilitate G-quadruplex formation and thus considered as potent G-quadruplex ligands. [21].

2.2 An Introduction to DNA

An important characteristic of a DNA molecule is the unique composition of twisted chains of a double polynucleotide in a double helical form around each other (Figure 2.1). Turning this design by 180°, superficially, the double helical structure remains the same. This unchanged structure can be explained based on the 2 DNA strands' complementary essence. Phosphate residues and sugar units made up each helical backbone of the strands and bases stick inward, which are approachable via the minor or major grooves.
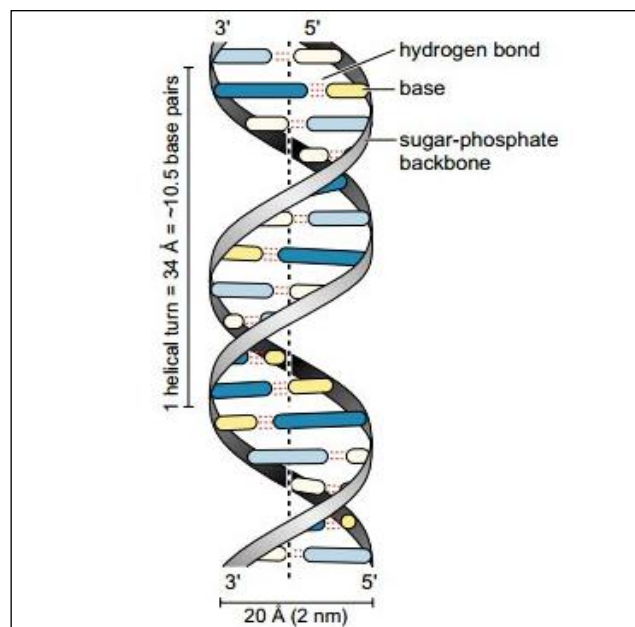
Figure 2.1: Schematic representation of a double helical DNA [22].

Nucleotides are the main structure of deoxyribonucleic acids. Nucleotides are made up of a sugar called deoxyribose, a phosphate, and a base. The sugar is linked to the base. The structure of sugar and phosphate is presented in Figure 2.2.
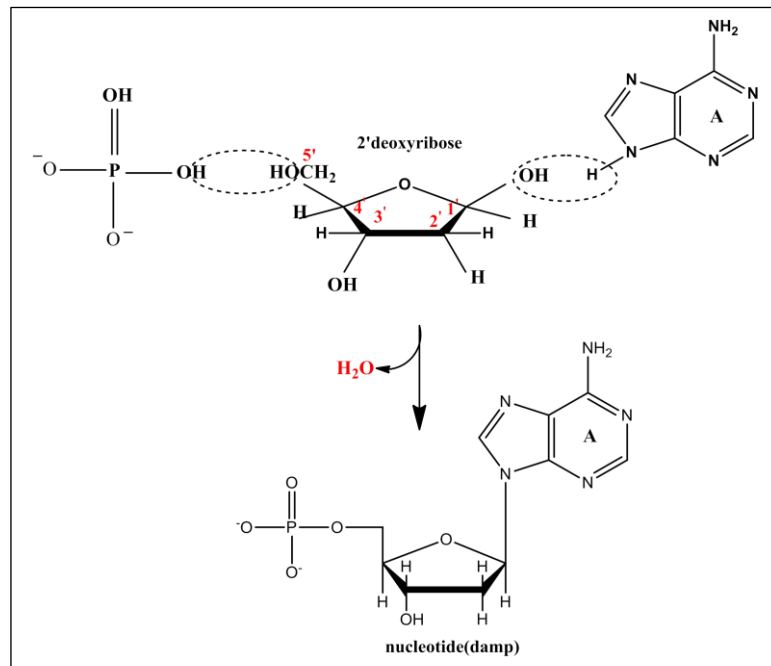
Figure 2.2: The structure of sugar and phosphate [22].

2'-deoxyribose is the name of the sugar; since it does not have a hydroxyl group at position 2' (Figure 2.2) and relatively contains two hydrogen atoms. A broad analysis about the linkage between the base and the 2'-deoxyribose are done. The elimination of water molecules from the base and the 1' sugar carbon is done which yields a glycosidic linkage. Nucleoside is the summation of the base and sugar. Likewise, removing a water molecule between the hydroxyl on the carbon at 5' position of 2'-deoxyribose and phosphate groups generate a phosphomonoester linkage. Addition of phosphates to nucleosides yields nucleotides. Nucleotide was produced by glycosidic linkage between the sugar with the base and phosphoester linkage between the phosphoric acid and the sugar. Bridging is formed when numerous nucleotides come together, which leads to the formation of a polynucleotide.

Deoxyribonucleic bases can be classified as follows; pyrimidines and purines. A (Adenine) and G (guanine) constitute the purine bases while C (cytosine) and T

5

(thymine) constitute the pyrimidine bases. Figure 2.3 represents some core structures of the deriving purines, which are a double ring, but pyrimidine just bear one core. Variations on a single ring lead to T and C as illustrated in the figure. Furthermore, numbering is visualized on the core structures of purines and pyrimidines accompanying its numbering format. Glycosidic linkages or bridges attach bases on to deoxyribose at the N1 position at the core of pyrimidine or on the N9 position on the purine core.
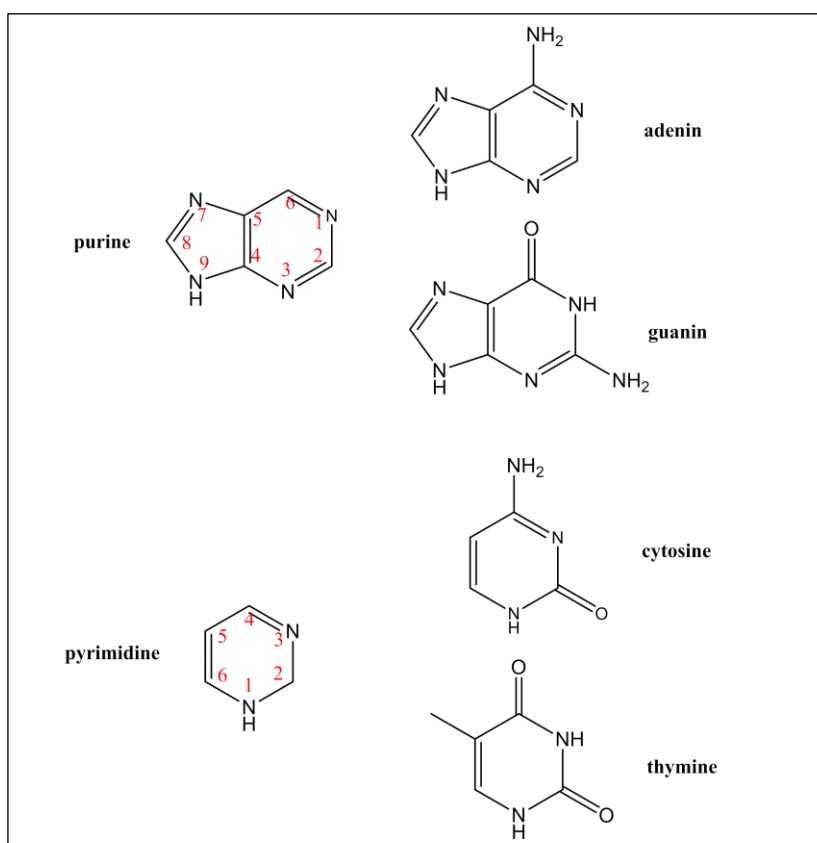
Figure 2.3: The structure of cores of Purine and Pyrimidine bases [23].

Two chains of polynucleotides made up the double helical structure of DNA that is bridged together by non-covalent, weak linkages between the base pairs. Adenine of a complimentary strand always bonds with T on another strand; likewise, C always bonds with G. Opposite bases pairing hold two stranded helical DNA geometries

together. Base pairing is done in this order 5' to 3' of two different strands. An anti-parallel preference exists between the two strands. This is the consequence of stereochemistry of A-T and G-C pairing [23-24].

Guanine quadruplex is a tertiary nucleic acid design composed of two or numerous guanine quartets paired that stack on each other. This design is represented in the following figure.
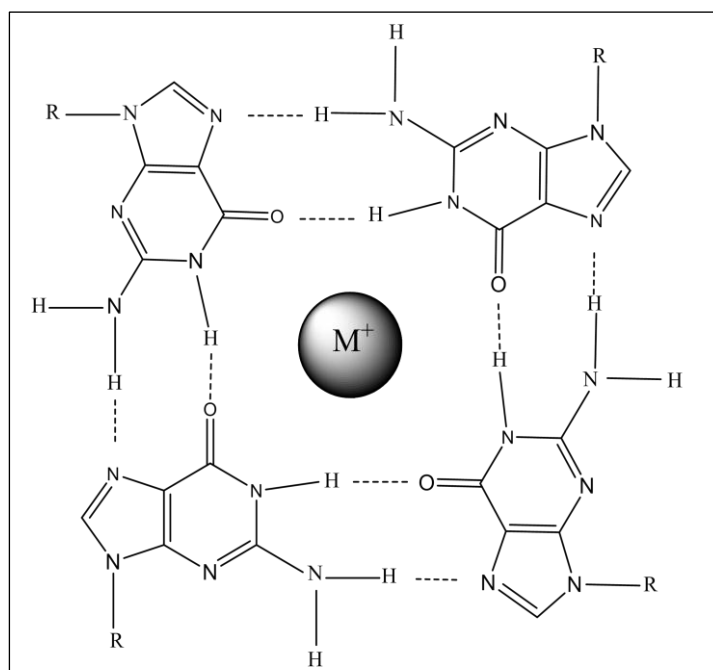
Figure 2.4: The structure of a guanine quartet [25] .

Four guanine bases (G) that linked by eight Hoogsteen hydrogen bridges (represented in the Figure 2.4 by dotted lines) leads to the formation of a guanine quartet. M^+ is a metal ion coordinated to six oxygen atoms of G within a quartet. Guanine quadruplexes outcome as a result of stacking of numerous guanine quartets on each other. It is well known that guanine quadruplexes play an essential role in gene expression regulations and telomeric length maintenance. Telomerase enzyme functions can be stopped with the creation of a quadruplex at the end of a telomere. Guanine quadruplex has a completely different structure, as a result of strand

directions, orientation of the loops, and the nature of metal cations which stabilize the quadruplex. Obviously guanine quadruplexes own unimolecular or bi and tetramolecular structures. Quadruplex strand orientation can be antiparallel or parallel in direction. The sequence and length of the intertwining of loops is of great importance for the creation and initiation of quadruplex structures' stabilities. Diverse conformations of guanine quadruplex can be assumed, although, they share a unique quartet planar structural feature, which creates a platform to create and stabilizes the quadruplex via small organic substances which stack at the top of the quartets [25].

The latter mentioned results by considering the peroxidase-like characteristic of a hemin-guanine-quadruplex complex. The key focus here is the binding of specific guanine quadruplex to hemin. The reason is the fact that; the system cannot work if hemin binds to a ssDNA and dsDNA nonspecifically and the complexes further exert peroxidase-like character. π-conjugated cationic molecules e.g. cationic porphyrin bind with guanine quadruplexes through π- π interactions with guanine quartets and through electrostatic interactions with guanine quadruplexes possessing anionic phosphate groups. Most often, the specificity owns lower quantities due to the electrostatic interaction, which is similarly reasons of binding non-specificity to ssDNA and dsDNA. On the other hand, hemin binding specificity in comparison to guanine quadruplex is remarkably higher. The specificity is for an electrostatic repulsion between phosphate groups of the deoxyribonucleic acid and the hemin carbonyl groups which results in the prevention of the hemin bind with dsDNA and ssDNA. As a counter reaction to the electrostatic repulsion, the huge hemin π-planar can create π-π stacking activity with guanine quartets of guanine quadruplex by neglecting its electrostatic repulsion. In addition, different ligands have been

synthesized that contain great π-planar structures and functional cationic groups for creating stable π-π stacking and electrostatic interactions with G-quadruplex. One of the most important guanine quadruplex ligands possessing characteristics similar to TMPyP4 (5,10,15,20-tetra-(N-methyl-4-pyridyl) porphine), which is a cationic porphyrin derivative made up of 4 pyrrol groups with 4 functional cationic groups. However, TMPyP4 bears the positive charges mediate in the creation of nonspecific interactions with dsDNA. Considering the nonspecific binding of dsDNA, there seems to be a need for a novel model for planning guanine quadruplex ligand with higher level of selectivity over dsDNA as it is of great importance. A solution to the problem could be achieved by the creation of functional anionic groups into in the huge π-planar center which has the capability of performing electrostatic interactions with phosphate anionic groups on dsDNA. The huge π-planar center increases the linking of guanine quadruplex and the π- π stacking interactions. Carbonyl groups on anionic porphyrins, hemin and NMM are appropriate binders to human guanine quadruplex telomeres possessing high selectivity over dsDNA and ssDNA [26]. These structures are represented in Figure 2.5.
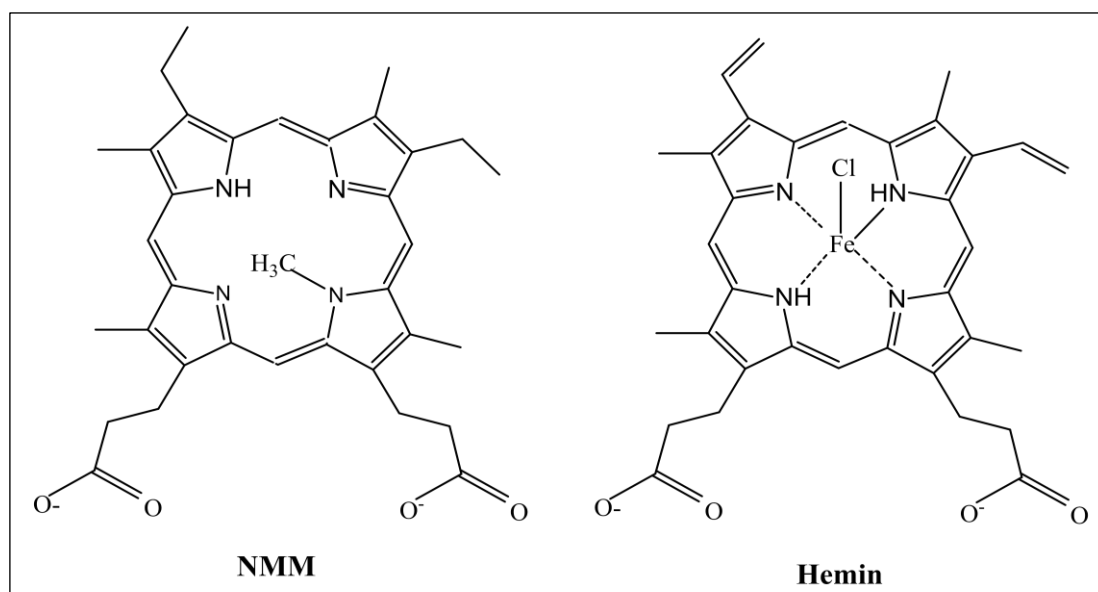

Figure 2.5: The structures of NMM and Hemin [26].

9

2.2.1 DNA – Binding Interaction

Separation and constitution of non-covalent interactions among various classes of macromolecules play a major role in the functionality of biological mechanisms. This phenomenon had been developed through three primary researches. An engineering combination of X-ray crystallography and genetics grants a coincident knowledge in regard to the association and structure of sequences of relevant acceptor ligand mechanisms [27]. Computer simulations and developmental science of interaction of macromolecules detect numerous varieties of microscopic atomic forces, bio-membrane probing, magnetique square and hydrodynamic techniques which lead to the experimental idea about the interaction of ligand-receptor bonding. Hydrogen bonding, π-π^* interactions, hydrophilic and hydrophobicity are temperature dependent and extremely weak bonds. Another factor is the steric hindrance that occur due to interaction between macromolecules and the system. These interactions are specifically depend on biological procedures relying on identification and molecular structures events. Binding among the two interacting components is based on entropy (-TΔS) and enthalpy (ΔH) dependency. This implies the fact that their identification relies on the identity of the dynamics and structure of each species. It is completely similar to any spontaneous process in which binding occurs while Gibbs free energy, ΔG of binding, is negative as a result of different thermodynamics driving the alternation of ΔH to $-$TΔS. Particularly, nuclear magnetic resonance (NMR), computation, and Isothermal Titrational Calorimetry (ITC) lead to the appraisal of donations of $-$TΔS and ΔH in free binding energy [28].

2.3 Naphthalene Dyes for Solar Cells

Nowadays, the various organic materials with the conjugated π-system are designed. They influence by energy levels including the band gaps unlike alkyl functional

groups. Measurements have proved that naphthalene is a line of compounds with n-type doping characterization. This implies that, n-type semiconductors are materials with high electron affinity and capability of accepting an electron [29].

The photophysical characterization of a molecular system that is of p- and n- types, is impressively determined by its environment and these properties do not belong to the nature of the molecule.

A solvent's influence is a key functionality that affects the photophysical properties of the substances, including its operational and processing conditions. P- and n- type materials demonstrate numerous desirable properties which are specified for organic electronic applications. A full characterization of a material's electrochemical, thermal, photochemical, and optical features leads to the revelation of these properties.
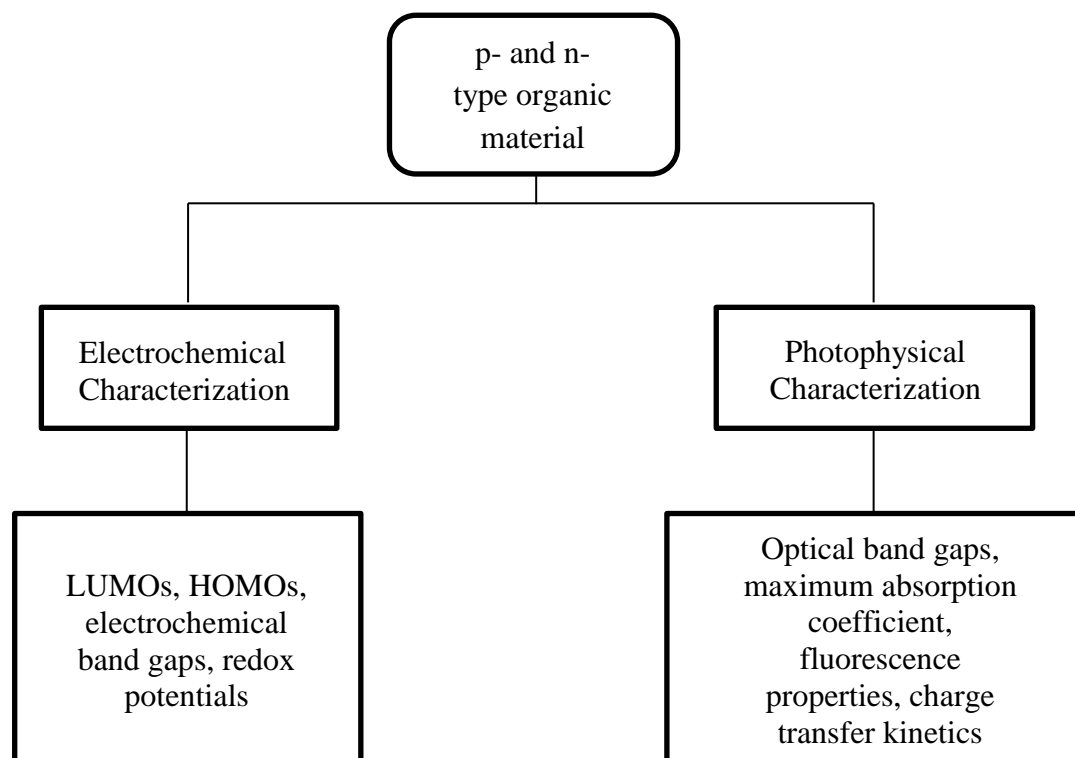
Figure 2.6: Characterization of p- and n-type materials

Electrochemical characterization of p- and n-type (Naphthalene) materials such as LUMOs, HOMOs, electrochemical band gaps, and redox potentials creates complete band structures of materials. This is advantageous in the identification of promising electron donors, relating to a structure for photovoltaic device designs. One desirable procedure to determine electrochemical parameters is to record squarewave, cyclic voltammograms of compounds through the implication of techniques of voltammetry. The cyclic voltammograms also display the attributed reversibility and electrochemical stabilities of the material [30].

2.4 Solar Cells

A solar cell is composed of a multi-layered unit that is produced as follows,Plastic or glass layer coating which serves as a protector to elements.Transparent Adhesive, this binds the glass and the other parts of a solar cell together. Anti-reflective covering; that prevents light striking the plate from bouncing off. This creates room for maximum absorption of energy inside the cell. Front Contact; transmitter of the electric current. N-type semiconductor; a thin silicon layer doped with phosphorous, which serves as a better conductor. P-type semiconductor layer; a thin silicon layer doped with boron to increase its conductivity.

Once the two conductive layers come in contact, a negative charge is created on the p-layer while a positive charge is created on the n-layer sections. This creates an imbalanced charge nature at the n-p junction which produces an electric square between the two layers, that is n- and p- layers. As radiant energy from the sun hits the electrons in the p-n junction, it gives them energy and pushes them to lose their host (atoms). The n-layer, which is positively charged, then attracts these electrons while at the same time the p-layer, which is negatively charged, repels them. A

12

circuit may be formed by connecting a wire to link the two layers (n- and p-).
Repulsion occurs between these electrons as they migrate into the n-layer, resulting
from a push due to the radiant energy. The connected wire serves as a bridge for
electrons to flow from one layer to the other. The flow of electrons creates an electric
current that is evident. The cell's electric field creates a voltage while the electron
flow creates the current. A product of both the voltage and current generates power
[31].
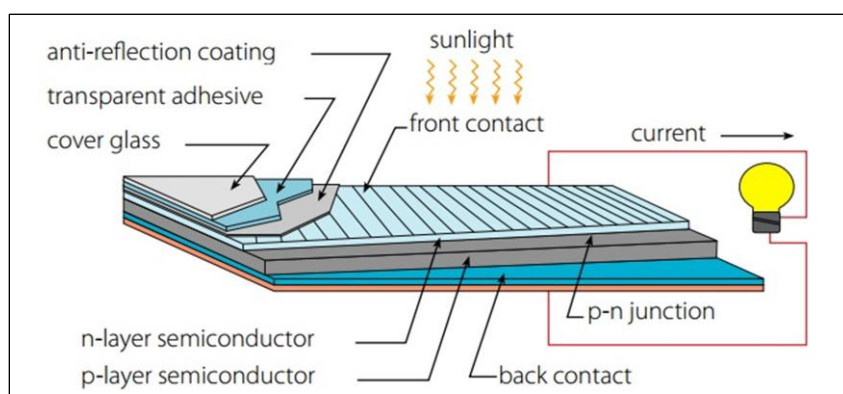
Figure 2.7: Concept of solar cells [32]

Unlike p-types, less amount of development is witnessed in n-type organic materials.
They are different from their molecular designs with the p-type semiconductors. In
molecular design focus, designing a material with electron poor characterization (e.g.
NDI) are difficult in comparison to designing an electron rich (p-type) materials.
Earlier n-type materials have shown undesirable properties such as poor stabilities in
light, trouble in synthesis, and poor solubility. This motivated researchers on the
production of high performance materials for applications in organic devices. A great
number of materials are employed as n-type substances in photovoltaics device such
as polymers. The base of these polymers are hydrocarbons with electron-

withdrawing functional groups such as nitro or cyano groups, the most popular fullerene, perylene, and naphthalene derivatives [32].

Chapter 3

EXPERIMENTAL

3.1 Chemicals and Instruments

3.1.1 Chemicals

1,4,5,8-napthalenetetracarboxylic dianhydride, tyramine, zinc acetate, m-cresol and isoquinoline were bought from Aldrich, a Company in Germany. The chemicals bought were in their purified state. Common organic solvents were distillated with respect to standard literature procedures [3-4]. As concerned with spectroscopy, spectroscopic solvents of pure grades were used directly.

3.1.2 Instruments

Ultraviolet Absorption Spectra

Varian Cary-100-Spectrometer was used to measure ultraviolet spectra in solutions.

Infrared Spectra

An infrared spectra was obtained from JASCO FT-IR-6200 Spectrometer by using solid KBR pellets.

Emission Spectra

Varian-Cary-Eclipse-Fluorescence spectrometer was used to study the emission spectra and fluorescence quantum yield of the synthesized compounds.

3.2 Synthetic Method of Naphthalene-imide ligands

The synthetic method of N,N'-Bis(2-(4-hydroxyphenyl)ethyl)-1,4,5,8-naphthalenediimide (HE-NDI) is shown in Scheme 3.1.

The product was synthesized successfully according to our procedure described in literature [3].
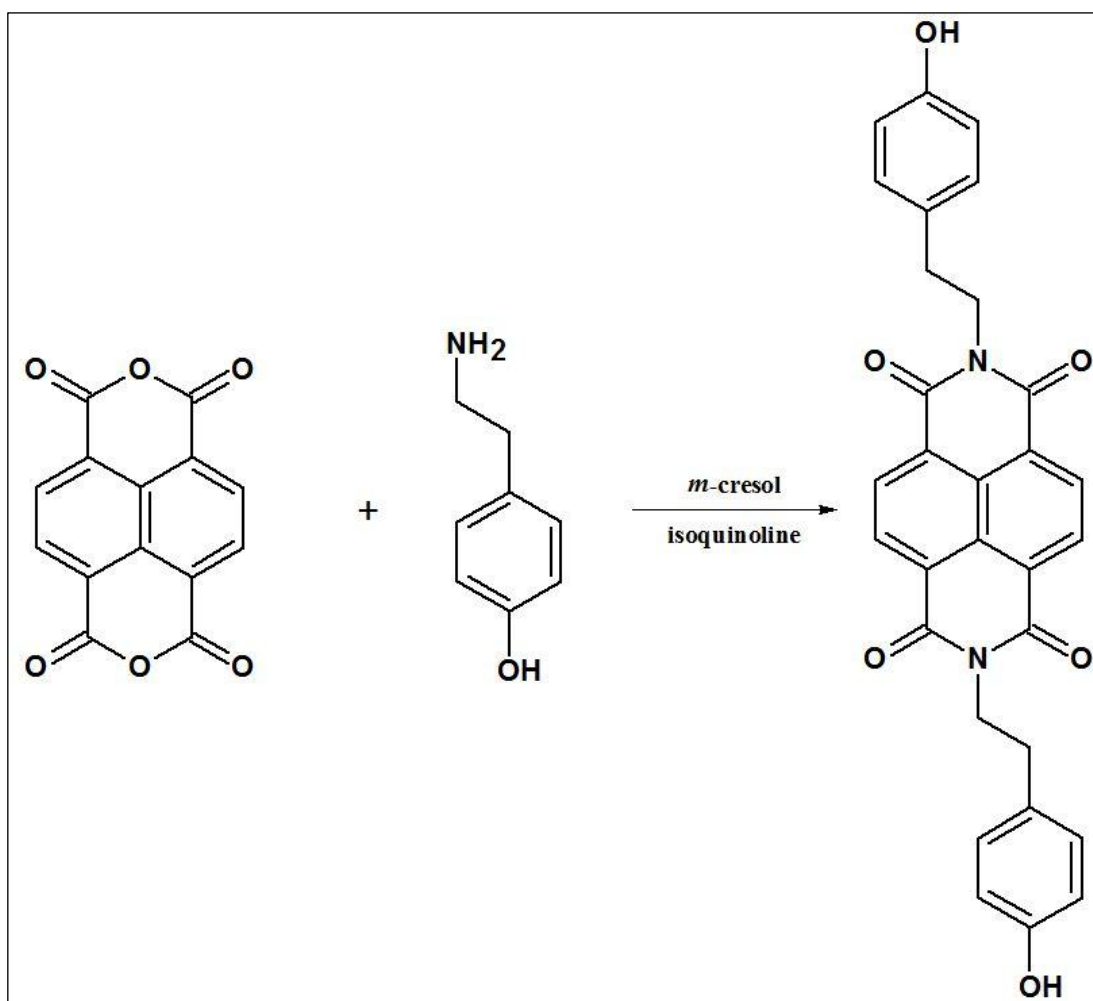
Scheme 3.1: Synthetic route of HE-NDI.

3.2.1 Synthesis of HE-NDI
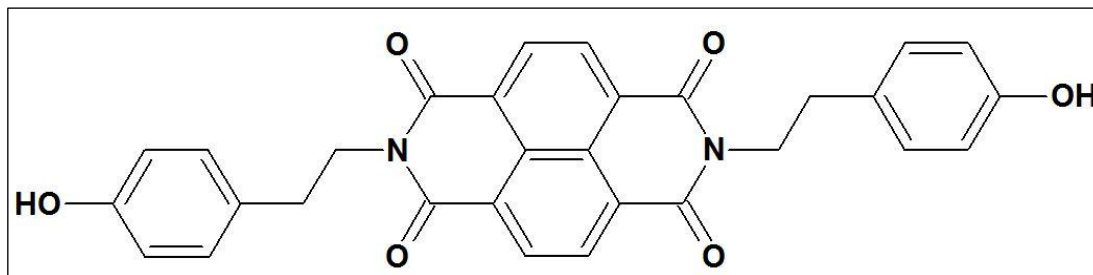
A suspension of NDA (1.003 g, 3.74 mmol), Tyramine (1.286 g, 9.37 mmol), and Zinc Acetate (0.828 g, 3.77 mmol) in solvent mixture (m-cresol and isoquinoline, 40:10) was stirred under argon atmosphere at room temperature. The reaction mixture was further stirred at 80 °C for 1 hour, 180 °C for 3 hours and 200 °C for 4 hours. The reaction mixture was allowed to cool to room temperature and poured into 500 mL ethanol. The product was treated with ethanol in a Soxhlet apparatus for 24 hours in order to remove the zince acetate and high boiling solvents.

Yield: 92.40% (1.750 g); **Color:** yellow, **Melting point >** 300°C

**FT-IR (KBr, cm^{-1}):** υ = 3345, 3068, 3022, 2975, 1700, 1655, 1583, 1511, 1456, 1372, 1335, 1261, 1224, 1168, 1112, 1016, 890, 834, 760, 573, 524.

UV-Vis (DMF) (λ_{max} / nm (ε_{max} L.mol^{-1}.cm^{-1})): 343 (70000), 360 (110000), 381 (120000).

Fluorescence (DMF) (λ_{max} nm): 534, 564; Φ_f = 0.30

3.3 General Reaction Mechanism of Naphthalene Dyes

Step 1 :
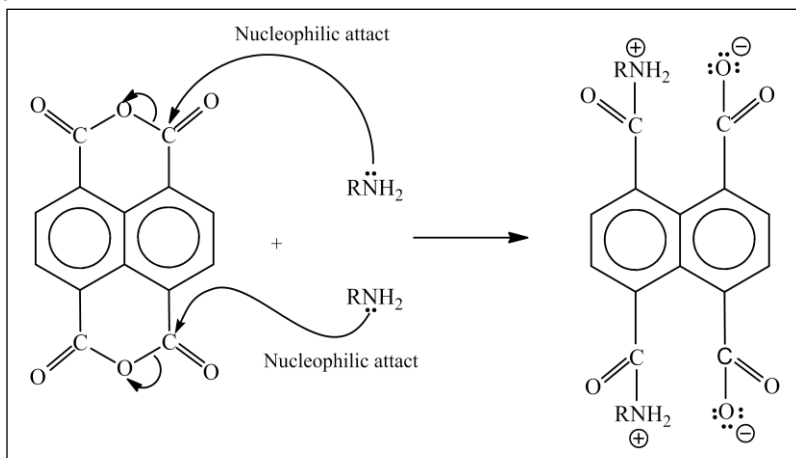
Step 2 :

Step 3:

Step 4 :

Step 5 :

19
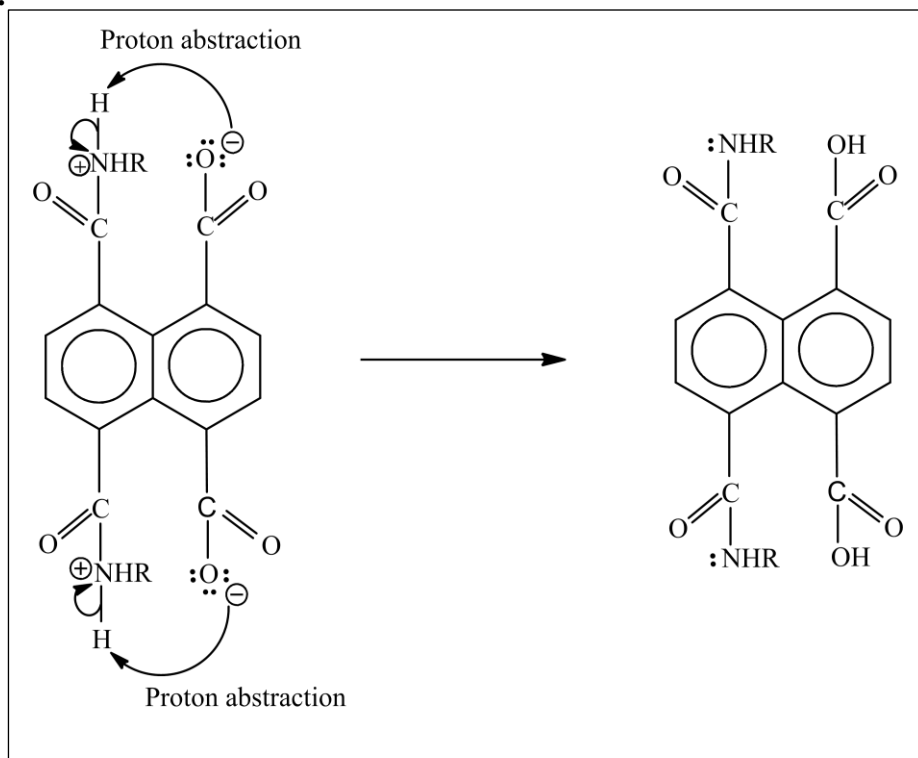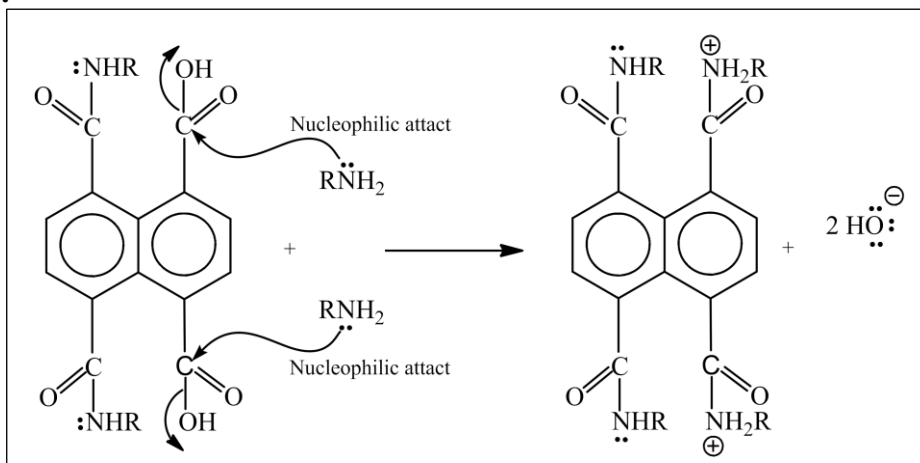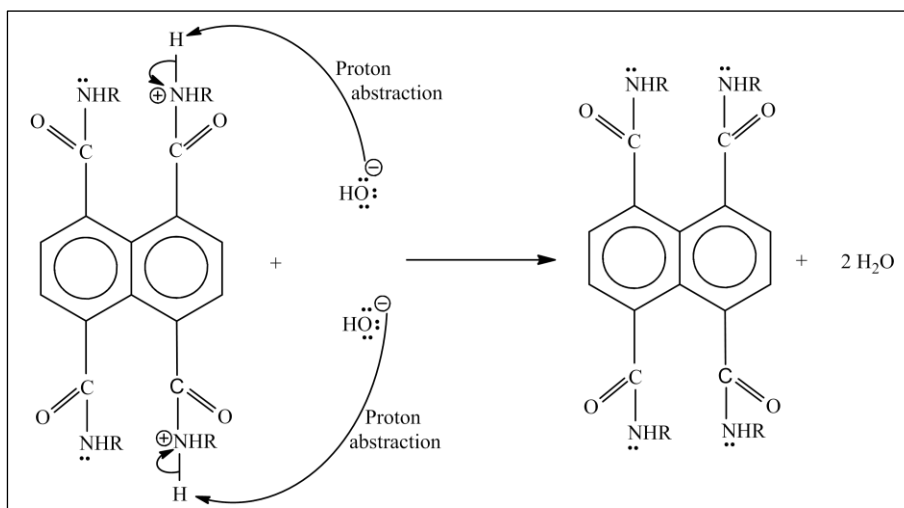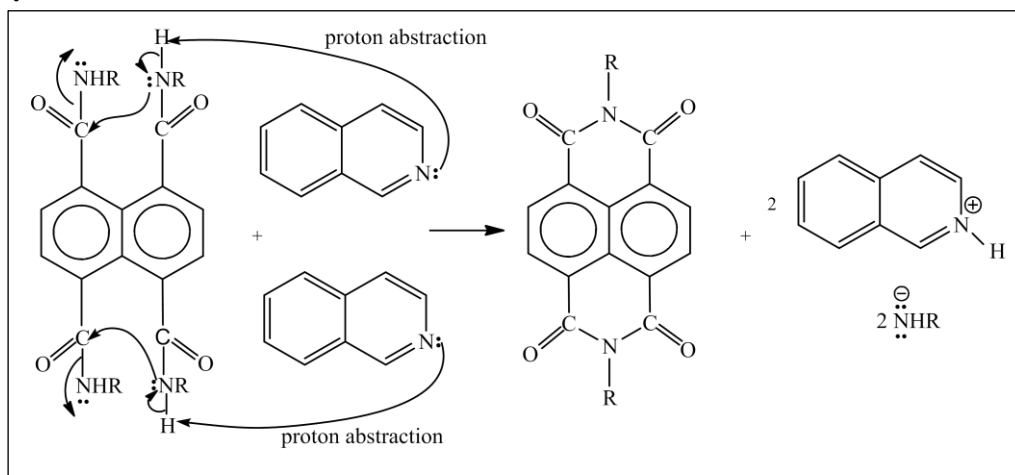
Step 6 :

Chapter 4

DATA AND CALCULATION

4.1 Fluorescence Quantum Yield (Φ_f)

Fluorescence is the major radiative procedure that the deactivation of energy happens through emission of a photon. Lossing of energy like heat to the surrounding is related to non-radiative procedure.

The fluorescence quantum yield of HE-NDI was calculated by using the equation 4.1 give bellow.

$$\Phi_f\,(U) = \frac{A_{std}}{A_u} \times \frac{S_u}{S_{std}} \times \left[\frac{n_u}{n_{std}}\right]^2 \times \Phi_{std} \qquad (Eq.4.1)$$

$\Phi_f(U)$: Fluorescence quantum yield of unknown

A_{std} : Absorbance of the reference at the excitation wavelength

A_u : Absorbance of the unknown at the excitation wavelength

S_{std} : The integrated emission area across the band of reference

S_u : The integrated emission area across the band of unknown

n_{std} : Refractive index of reference solvent

n_u : Refractive index of unknown solvent

Φ_{std} : Fluorescence quantum yield of reference

Φ_f of HE-NDI in DMF:

Anthracene was used as reference in measurements (λ_{max} = 360 nm, Φ_f = 0.27) [3].

Φ_{std} = 0.27 in ethanol

A_{std} = 0.1022

A_u = 0.11

S_u = 4551.87

S_{std} = 4200.55

n_{std} = 1.3617

n_u = 1.428

$$\Phi_f = \frac{0.1022}{0.11} \times \frac{4551.87}{4200.55} \times \left[\frac{1.428}{1.3617}\right]^2 \times 0.27$$

Φ_f = 0.30

4.2 Molar Absorption Coefficients

The molar absorption coefficients were calculated through the equation 4.2 known as Beer-Lambert Law.

$$\boldsymbol{\varepsilon_{max} = \frac{A}{cl}} \qquad \textbf{(Eq.4.2)}$$

Where

ε_{max} : Molar absorption coefficient at concentration of 1×10^{-5} M

A : Absorbance

l : Cell length

c : Concentration in mol.L^{-1}

22
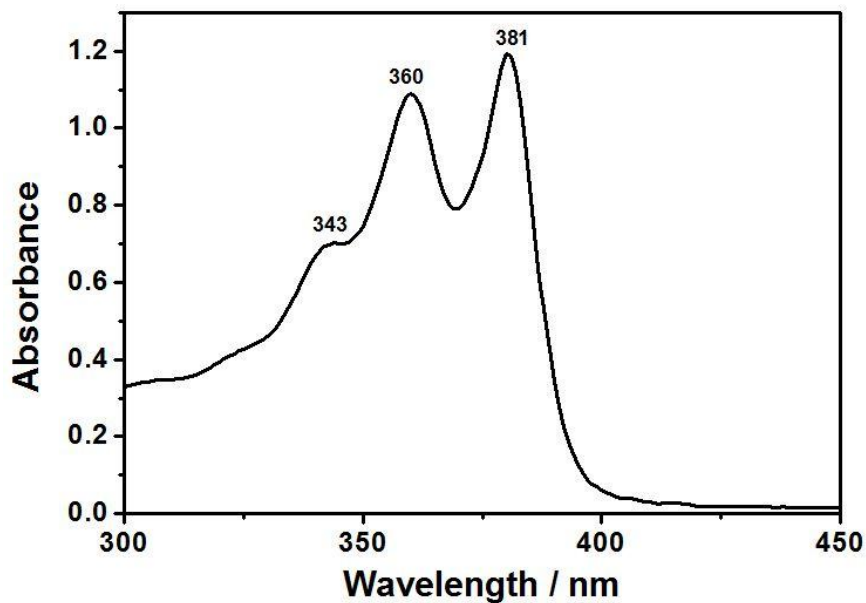
ε_max of HE-NDI in DMF:

Figure 4.1: Absorption Spectrum of DMF in 1×10^{-5} M

$$\varepsilon_{max} = \frac{1.1927}{1\times10^{-5}\,M \times 1cm} = 119270 \text{ L.mol}^{-1}.\text{cm}^{-1}$$

Table 4.1: Molar absorptivity data of HE-NDI in DMF and CHL

Solvent	Concentration	Absorbance	λ_{max} (nm)	ε_{max} (L.mol^{-1}.cm^{-1})
DMF	1×10^{-5} M	1.1927	381	119270
CHL	1×10^{-5} M	0.7178	381	71870

4.3 The Half-width of the Selected Absorption ($\Delta\bar{v}_{1/2}$)
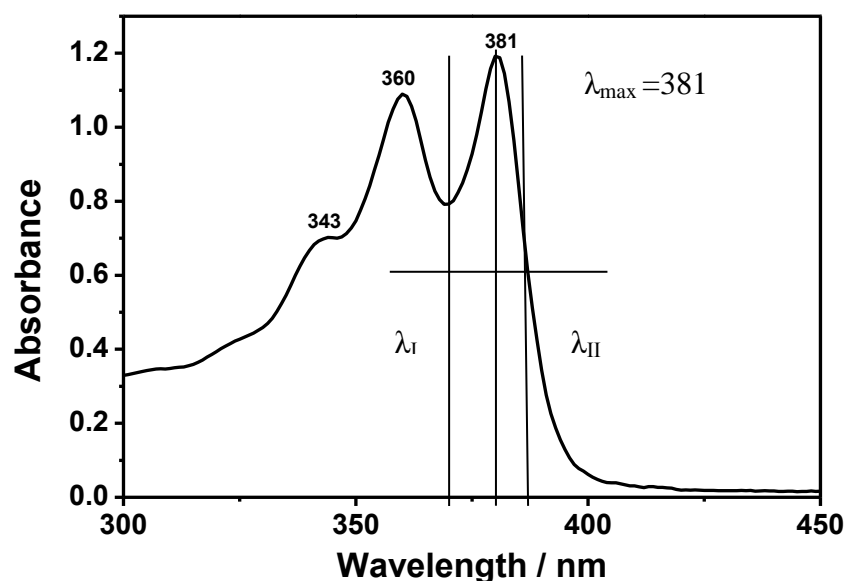
Figure 4.2: Absorption Spectrum of HE-NDI in DMF for the Half - width calculation

$$\Delta\bar{v}_{1/2} = \bar{v}_{II} - \bar{v}_{I} \qquad\qquad \textbf{(Eq.4.3)}$$

λ_I = 369 nm

$$369 \text{ nm} \times \frac{10^{-9} \text{ m}}{1 \text{ nm}} \times \frac{100 \text{ cm}}{1 \text{ m}} = 3.69 \times 10^{-5} \text{ cm}$$

$$\bar{v}_I = \frac{1}{\lambda_I} = \frac{1}{3.69 \times 10^{-5} \text{cm}} = 27100.27 \text{ cm}^{-1}$$

λ_{II} = 389 nm

$$389 \text{ nm} \times \frac{10^{-9} \text{ m}}{1 \text{ nm}} \times \frac{100 \text{ cm}}{1 \text{m}} = 3.89 \times 10^{-5} \text{ cm}$$

$$\bar{v}_{II} = \frac{1}{3.89 \times 10^{-5} \text{cm}} = 25706.94 \text{ cm}^{-1}$$

$$\Delta\bar{v}_{1/2} = \bar{v}_{II} - \bar{v}_I = 27100.27 - 25706.94 = 1393.33 \text{ cm}^{-1}$$

Table 4.2: Half-width data ($\Delta\bar{\upsilon}_{1/2}$) of HE-NDI in DMF and CHL

Solvent	λ_{max}	λ_I	λ_{II}	$\upsilon_I(cm^{-1})$	$\upsilon_{II}(cm^{-1})$	$\Delta\bar{\upsilon}_{1/2}(cm^{-1})$
DMF	381	369	389	27100.27	25706.94	1393.33
CHL	381	369	387	27100.27	25839.79	1260.48

4.4 Theoretical Radiative Lifetimes (τ_0)

τ_0 was calculated using the equation 4.4 shown below [33].

$$\tau_0 = \frac{3.5 \times 10^8}{\bar{\upsilon}^2_{max} \times \varepsilon_{max} \times \Delta\bar{\upsilon}_{1/2}} \qquad \textbf{(Eq.4.4)}$$

Where

τ_0 : Theoretical radiative lifetime in seconds

$\bar{\upsilon}_{max}$: Wavenumbers in cm^{-1}

ε_{max} : The maximum extinction coefficient at the selected adsorption wavelength

$\Delta\bar{\upsilon}_{1/2}$: Half-width of the selected absorption in units of cm^{-1}

τ_0 of HE-NDI in DMF :

λ_{max} = 381 nm

$$\lambda_{max} = 381nm \times \frac{10^{-9}m}{1nm} \times \frac{100cm}{1m} = 3.81 \times 10^{-5}cm$$

$$\bar{\upsilon}_{max} = \frac{1}{\lambda_{max}} = \frac{1}{3.81 \times 10^{-5}\ cm} = 26246.71\ cm^{-1}$$

$$\bar{\upsilon}^2_{max} = (26246.71\ cm^{-1})^2 = 6.889 \times 10^8 cm^{-2}$$

$$\tau_0 = \frac{3.5 \times 10^8}{6.889 \times 10^8 cm^{-2} \times 119270 \times 1393.33 \times cm^{-1}} = 3.0572 \times 10^{-9}sec$$

$$\tau_0 = 3.057 \times 10^{-9}sec \times \frac{1ns}{10^{-9}sec} = 3.06\ ns$$

Theoretical radiative lifetimes calculated in DMF and CHL were tabulated in Table 4.3.

Table 4.3: Theoretical radiative lifetimes of HE-NDI in DMF and CHL

Solvent	λ_{max}	ε_{max} ($L.mol^{-1}.cm^{-1}$)	$\bar{\upsilon}^2_{max}$ (cm^{-2})	$\Delta\bar{\upsilon}_{1/2}$ (cm^{-1})	τ_0 (ns)
DMF	381	119270	6.889×10^8	1393.33	3.06
CHL	381	71870	6.889×10^8	1260.48	5.61

4.5 Theoretical Fluorescence Lifetime(τ_f)

τ_f value of HE-NDI was calculated using the equation 4.5 shown below [33].

$$\tau_f = \tau_0 . \Phi_f \qquad \textbf{(Eq.4.5)}$$

Where

τ_f : Fluorescence lifetime (ns)

τ_0 : Theoretical radiative lifetime (ns)

Φ_f : Fluorescence quantum yield

τ_f of HE-NDI in DMF:

$\tau_f = \tau_0 . \Phi_f$

$\tau_f = 3.06$ ns $\times 0.30 = 0.92$ ns

4.6 Theoretical Fluorescence Rate constant (k_f)

k_f value was calculated via Turro's equation 4.6 shown below.

$$k_f = \frac{1}{\tau_0} \qquad \textbf{(Eq.4.6)}$$

Where

k_f : Fluorescence rate constant (s^{-1})

τ_0 : Theoretical radiative lifetime (s)

k_f of HE-NDI in DMF:

$$k_f = \frac{1}{3.06 \times 10^{-9}} = 3.27 \times 10^8$$

The theoretical fluorescence rate constant of HE-NDI in DMF and CHL were shown in Table 4.4.

Table 4.4: Fuorescence rate constants results for HE-NDI in DMF and CHL

Solvent	τ_0 (ns)	k_f (s^{-1})
DMF	3.06	3.27×10^8
CHL	5.608	1.78×10^8

4.7 Oscillator Strengths (f)

The f value of HE-NDI was calculated using the equation 4.7 shown below [33].

$$f = 4.32 \times 10^{-9} \times \Delta\bar{\upsilon}_{1/2} \times \varepsilon_{max} \qquad \textbf{(Eq.4.7)}$$

Where

f : Oscillator strengths

$\Delta\bar{\upsilon}_{1/2}$: Half- width of the chosen absorption in unit of cm^{-1}

ε_{max} : The maximum extinction coefficient in L. mol^{-1}.cm^{-1} at the maximum absorption wavelength (λ_{max}).

Oscillator strengths of HE-NDI in DMF:

$f = 4.32 \times 10^{-9} \times \Delta\bar{\upsilon}_{1/2} \times \varepsilon_{max}$

$f = 4.32 \times 10^{-9} \times 1393.33 \times 119270 = 0.72$

The oscillator strengths of HE-NDI in DMF and CHL were shown in Table 4.5.

Table 4.5: Oscillator strengths of HE-NDI in DMF and CHL

Solvent	ε_{max} (L.mol^{-1}.cm^{-1})	$\Delta\bar{\upsilon}_{1/2}$ (cm^{-1})	f
DMF	119270	1393.33	0.72
CHL	71870	1260.48	0.39

4.8 Singlet Energy (E_s)

E_s of HE-NDI was calculated in DMF and CHL using the equation 4.8 shown below [33].

$$E_s = \frac{2.86 \times 10^5}{\lambda_{max}} \qquad \textbf{(Eq.4.8)}$$

Where

E_s : Singlet energy in kcal mol^{-1}

λ_{max} : The maximum absorption wavelength in Å

E_s of HE-NDI in DMF:

$$\lambda_{max} = \frac{2.86 \times 10^5}{3810} = 75.06 \text{ kcal mol}^{-1}$$

Table 4.6: Singlet energy data of HE-NDI in DMF and CHL

Solvent	λ_{max} (nm)	E_s (kcal mol^{-1})
DMF	381	75.06
CHL	381	75.06

4.9 Optical Band Gap Energies (E_g)

E_g value of HE-NDI was calculated in DMF and CHL using the equation 4.9 shown below.

$$E_g = \frac{1240ev \, nm}{\lambda} \qquad\qquad \textbf{(Eq.4.9)}$$

Where

E_g : band gap energy in ev

λ : cut-off wavelength of the absorption band in nm and acquired by tracing the line

of the maximum absorption band to zero-absorbance as representation in Figure 4.3.

E_g of HE-NDI:

$$E_g = \frac{1240ev \, nm}{393 \, nm} = 3.155ev$$
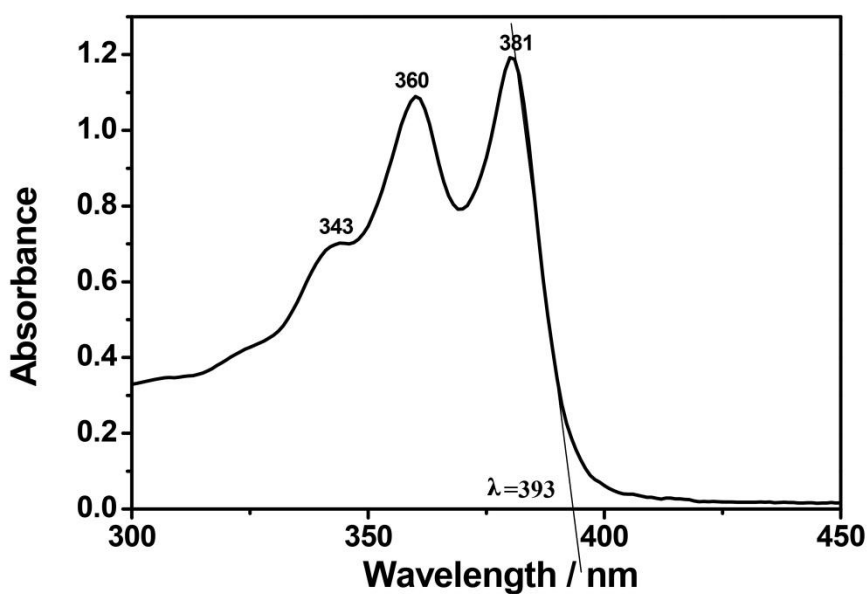
Figure 4.3: E_g calculation from the Absorption Spectrum of HE-NDI in DMF

Table 4.7: Optical Band Gap Energies for HE-NDI in DMF and CHL

Solvent	cut-off wavelength	E_g (ev)
DMF	393	3.155
CHL	388	3.195
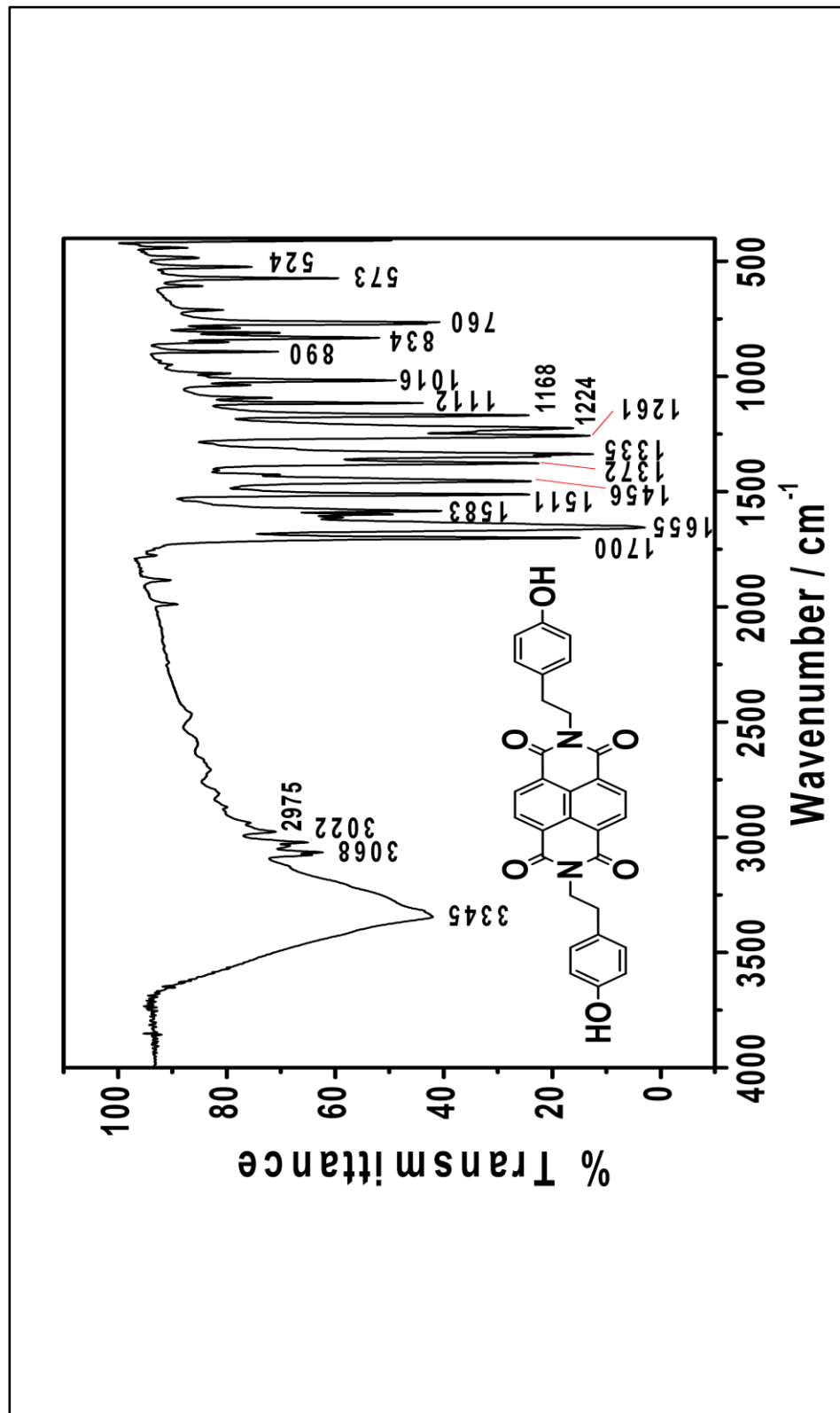
Figure 4.4: FT-IR Spectrum of HE-NDI
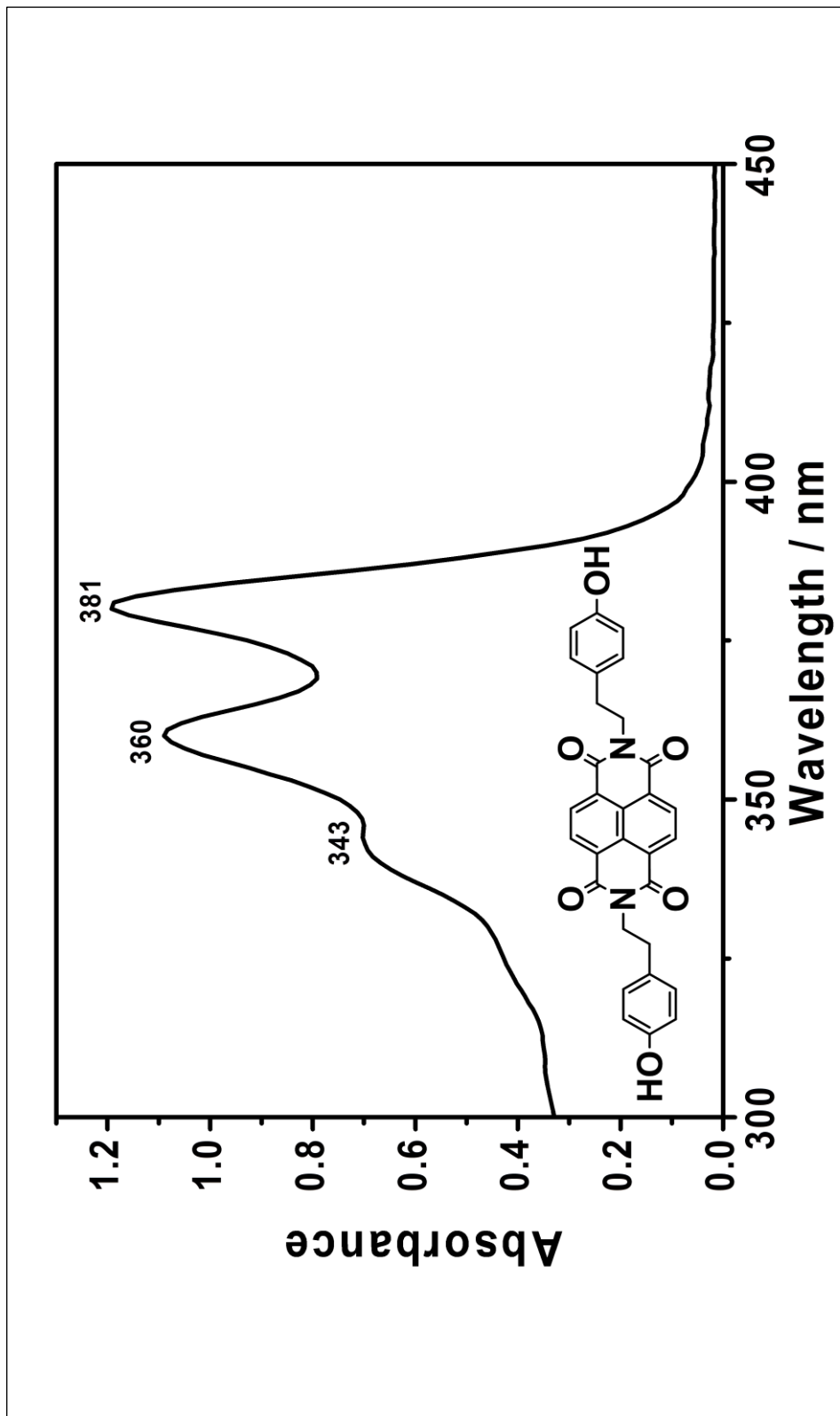
Figure 4.5: Absorption Spectrum of HE-NDI in DMF
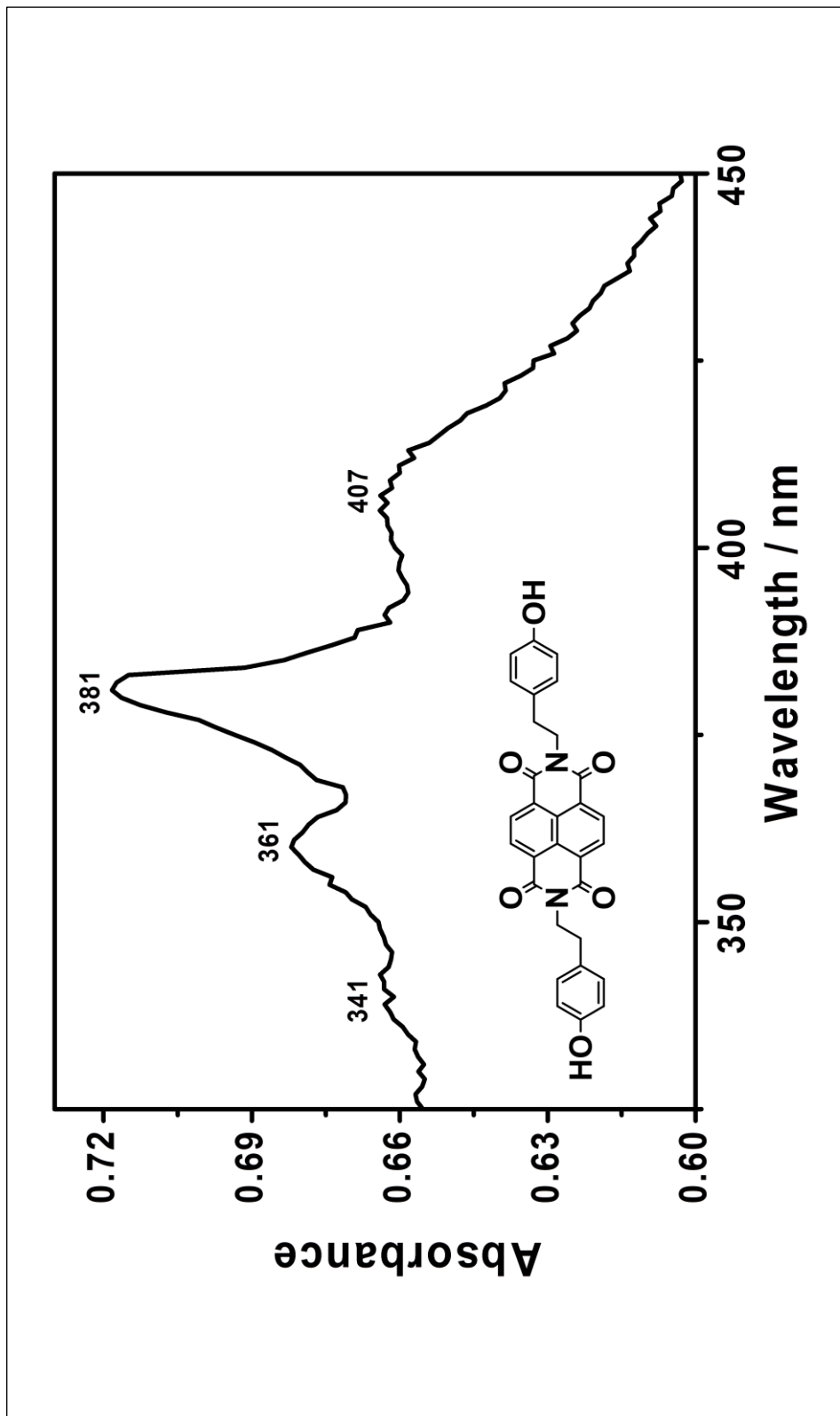
Figure 4.6: Absorption Spectrum of HE-NDI in CHL
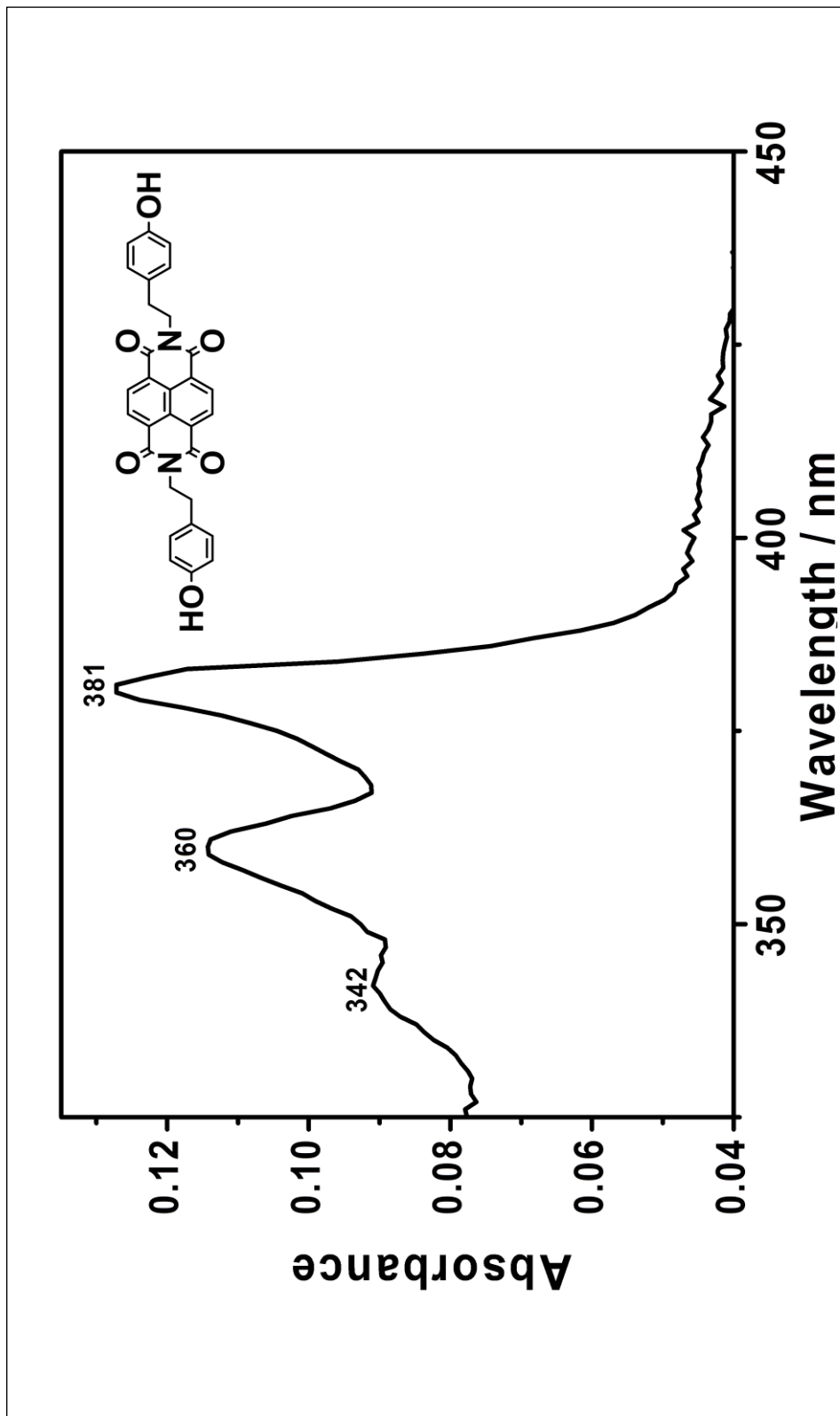
Figure 4.7: Absorption Spectrum of HE-NDI in CHL-MF
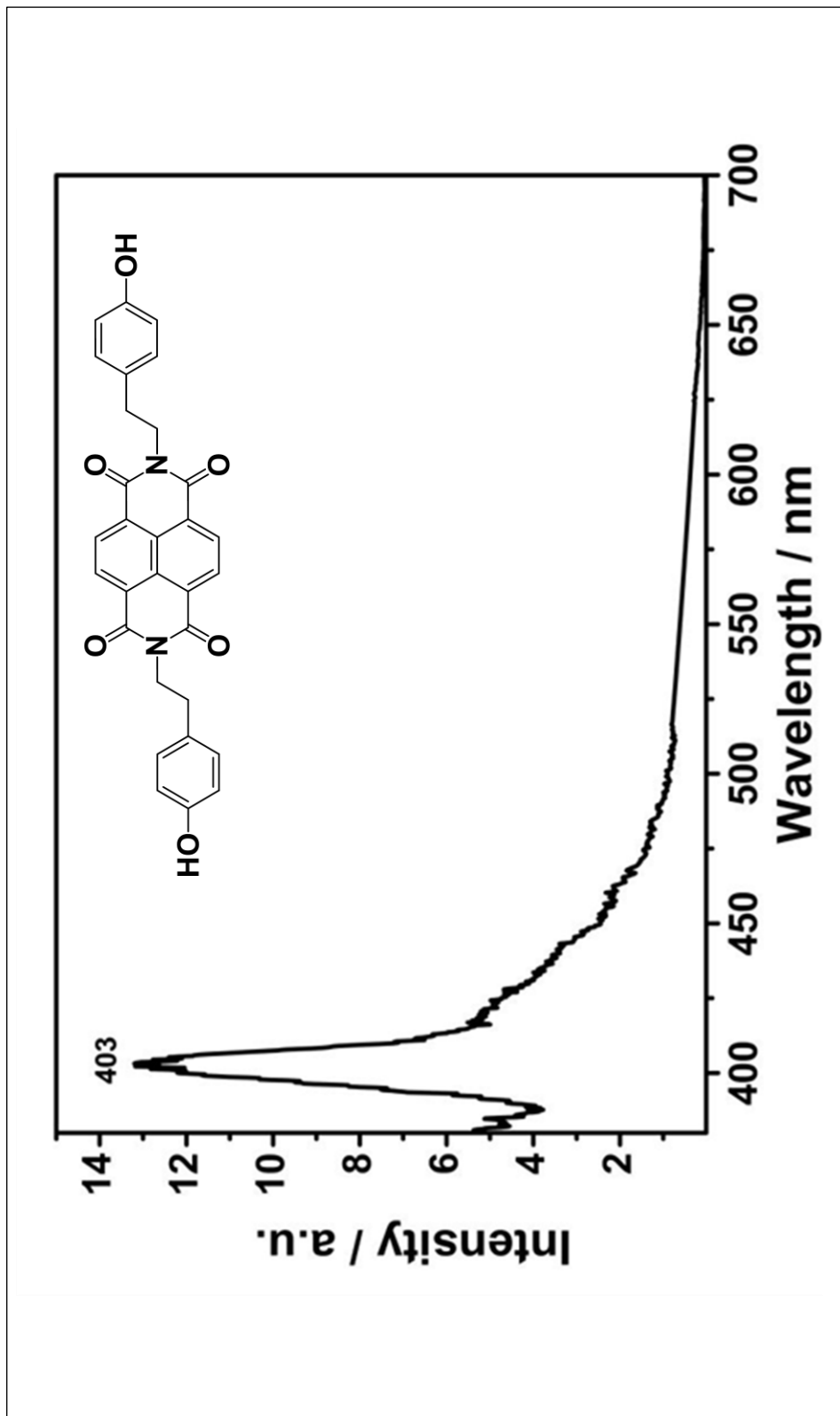
Figure 4.8: Emission Spectrum of HE-NDI in DMF
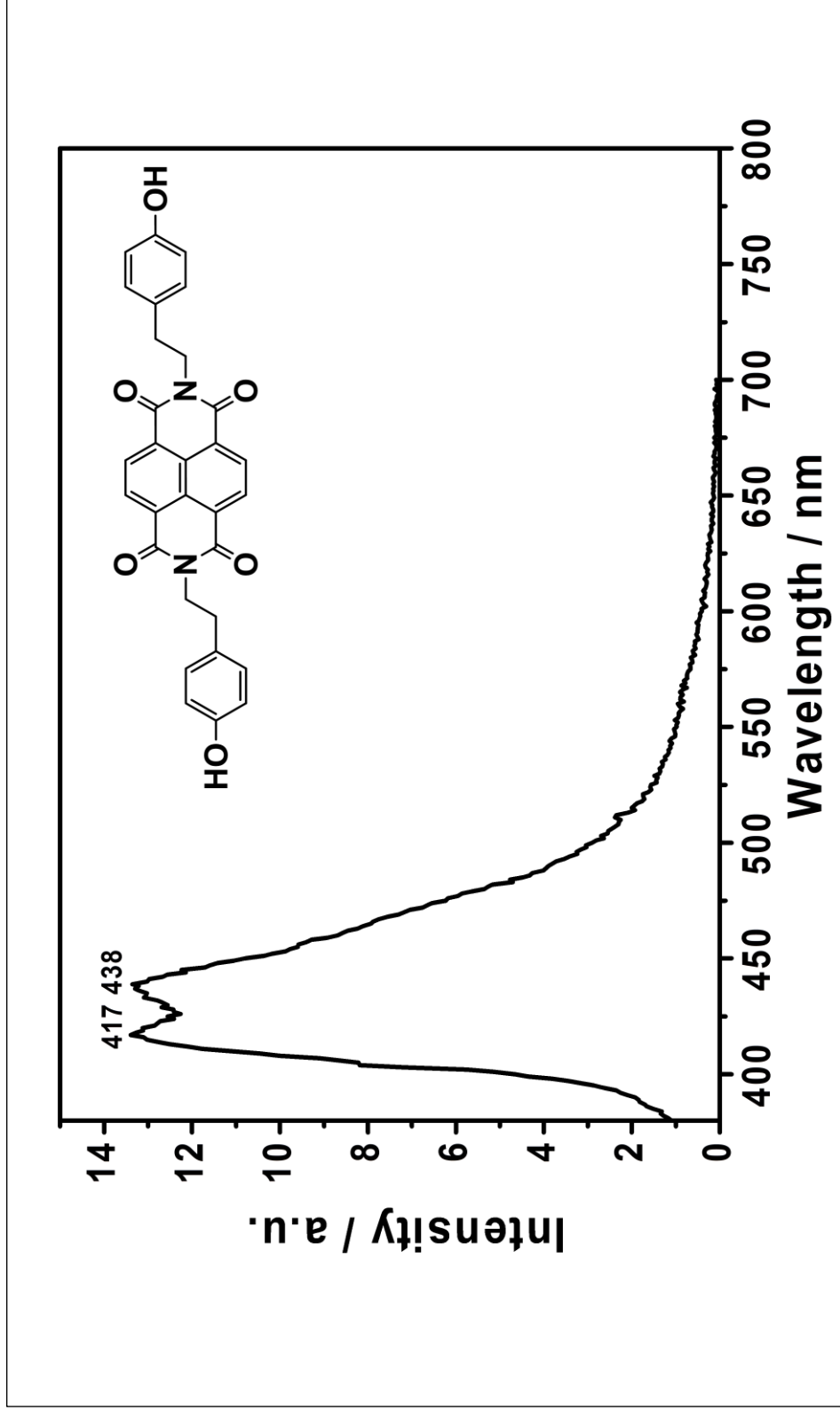
Figure 4.9: Emission Spectrum of HE-NDI in CHL
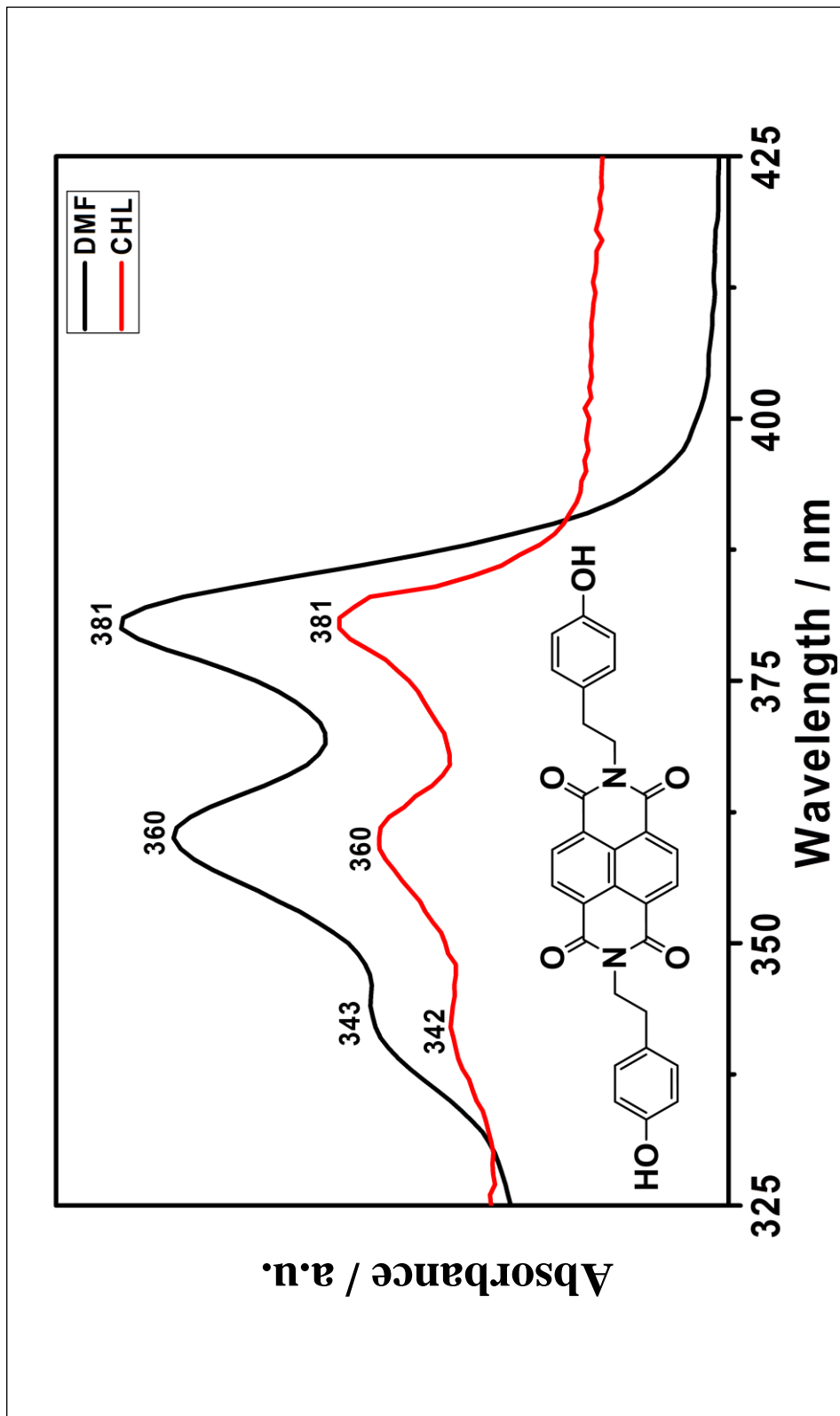
Figure 4.10: Absorption Spectra of HE-NDI in DMF and CHL
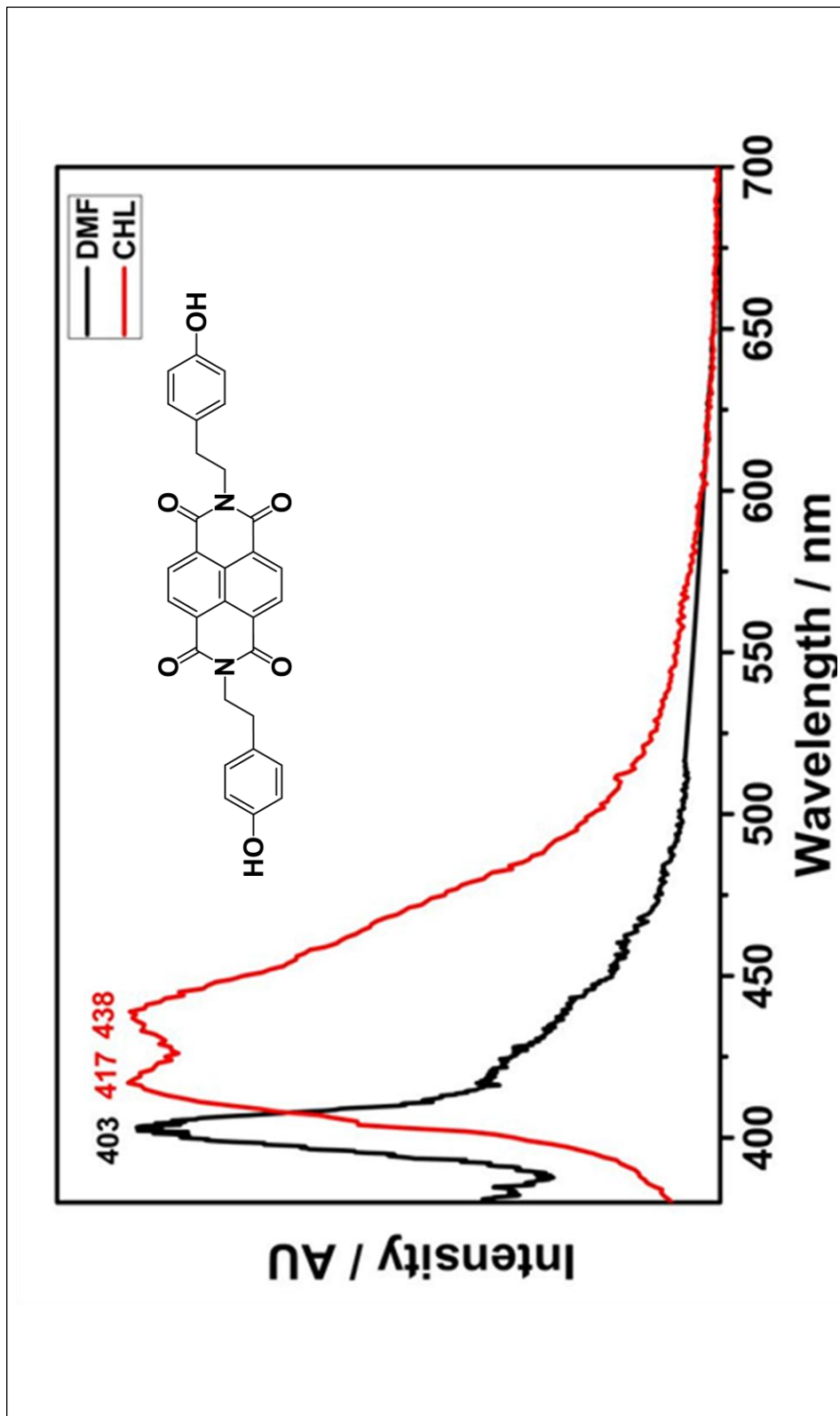
Figure 4.11: HE-NDI Emission Overlap in DMF and CHL
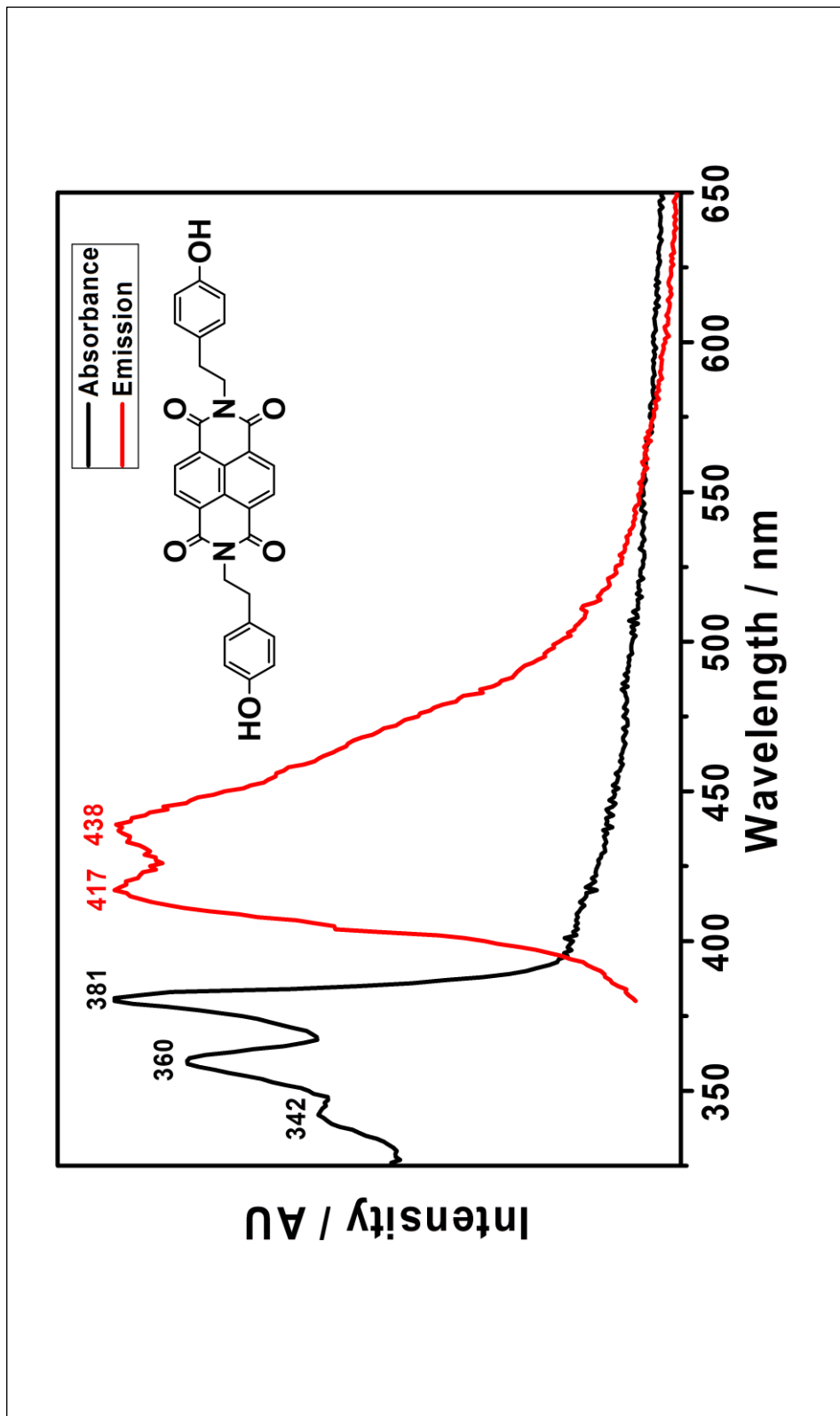
Figure 4.12: Comparision of Absorption and Emission Spectra of HE-NDI in CHL

Chapter 5

RESULT AND DISCUSSION

5.1 Synthesis of the Designed Naphthalene Dye

The novel naphthalene diimide, N,N'-Bis(4-hyroxyphenyl)-1,4,5,8-naphthalene diimide (HE-NDI) was successfully synthesized as shown in Scheme 3.1. The naphthalene diimide was synthesized in one step from 1,4,5,8-naphthalenetetracarboxylic dianhydride and Tyramine in isoquinoline and m-cresol solvent mixture. The compound was characterized with FT-IR spectroscopy.

5.2 Solubility of HE-NDI

Depending on the substituent nature of naphthalene dyes, their solubilities may change [3]. HE-NDI is completely soluble in polar aprotic solvent like dimethylformamide (DMF). On the other hand, it is partialy soluble in nonpolar solvents like chloroform (CHL). The better solubility of synthesized naphthalene diimide in DMF can be assigned to higher polar characteristic of HE-NDI. The Table 5.1 shows the solubility of HE-NDI.

Table 5.1: The solubility of HE-NDI in DMF and CHL

Solvent	Solubility
DMF	(+ +) / Dark yellow
CHL	(− +) / Light yellow

(+ +): Completely soluble at RT, (− +): Partly soluble

5.3 FTIR Characterization

The FT-IR spectrum recorded of synthesized HE-NDI was shown in Figure 4.4. The IR spectrum of HE-NDI shows all the functional groups that confirms the structure of the compound.

From the FT-IR spectrum of Figure 4.4, O–H stretch at 3345 cm^{-1}. Aromatic C–H stretch at 3022 cm^{-1} and 3068 cm^{-1}, aliphatic C–H stretch at 2975 cm^{-1}, imide C=O symmetric and asymmetric stretch at 1700 cm^{-1} and 1655 cm^{-1} , conjugated C=C stretch at 1583 cm^{-1}, C–N stretch at 1456 cm^{-1}, C–O stretches at 1016 cm^{-1} and Aromatic C–H bending at 760 cm^{-1} and 834 cm^{-1} respectively. All of the above mentioned peaks confirm the structure of synthesized HE-NDI.

5.4 Optical Properties

5.4.1 Analyses of UV-vis Absorption Spectra

Figures 4.5, 4.6 and 4.7 display the UV-vis absorption spectra of HE-NDI in two solvents. Figure 4.5 illustrates the absorption spectra of HE-NDI in DMF with three maximum absorption peaks at 343, 360 and 381 nm and the maximum absorption coefficient (ε_{max}) of 119270 $L.mol^{-1} cm^{-1}$. These three maximum absorption peaks are relevant to π-π interaction characteristic of HE-NDI. Figure 4.6 shows three maximum peaks in chloroform at 343, 360 and 381nm and also one extra peak compared to spectrum in DMF at 407 nm which can be ascribed to intermolecular interaction of HE-NDI in chloroform due to formation of aggregation. Moreover, Figure 4.7 demonstrates absorption spectrum in chloroform after micro filtration. As shown in the absorbtion spectrum, the fourth peak at 407 nm is not observed. This explains the aggregation in CHL. The molar absorption coefficients of HE-NDI in two solvents at 381 nm was reported in Table 4.1. The high molar absorptivity of

conjugated compound explain the high absorption capacity due to the intense π-π^* transition in the UV-vis region. The high molar absorptivity of compound (ε_{max} = 119270 L.mol^{-1} cm^{-1}) at 381 nm in DMF is due to better solubility of HE-NDI in polar aprotic solvents compare to nonpolar solvent, chloroform.

5.4.2 Analyses of Fluorescence Spectra

All the emission spectra of HE-NDI were taken at excitation wavelength (λ_{exc}) of 360 nm and represented in Figures 4.8 and 4.9. The emission bands in DMF show one peak at 403 nm (Figure 4.8). Furthermore, the emission bands in CHL display two bands at 417 and 438 nm, respectively (Figure 4.9). Red shifted emissions can be seen from the emission spectra of HE-NDI in CHL solvent compared to the spectrum in DMF solvent. The relative fluorescence quantum yields were determined in DMF by using the anthracene as a standard (Equation 4.1). The fluorescence quantum yields of synthesized compound is measured as 0.30 in DMF. It is noteworthy that the fluorescence quantum yield of naphthalene dyes are generally less due to inter system crossing [6-7]. Additionally, the great Stoke shifts were observed in CHL solvent (Figure 4.12).

Chapter 6

CONCLUSION

The project is focused on the synthesis and characterization of novel N,N$^{'}$–bis(4-hyroxyphenyl)-1,4,5,8-naphthalenediimide (HE-NDI) for photonic applications and DNA bindings.

HE-NDI dye was synthesized successfully with high yields and its structure was confirmed by FT-IR spectroscopy. In order to explore their potential applications, a detailed characterization of optical and photophysical properties were performed.

HE-NDI was completely soluble in dimethylformamide (DMF). However, partially soluble in chloroform (CHL). The better solubility of synthesized naphthalene diimide in polar aprotic solvents assigned polar characteristic of HE-NDI.

The absorption spectra of HE-NDI in DMF and CHL showed three characteristic maximum absorption peaks at 343, 360 and 381 nm. The fourth peak in CHL belongs to aggregation.

The high molar absorptivity of compound (ε_{max} = 119270 L.mol^{-}.cm^{-1}) at 381 nm in DMF is resulting from strong inter and intramolecular interactions due to polar nature of DMF.

The emission band in DMF display one paek at 403 nm. Furthermore, the emission bands in CHL for HE-NDI are 417 and 438 nm, respectively (Figures 4.10). Red shifted emissions can be seen from the emission spectra of HE-NDI in CHL solvent compared to the DMF solvent.

The fluorescence quantum yield of compounds is calculated as 0.30 for HE-NDI in DMF.

Future Work

Finally, as mentioned in these studies the HE-NDI has the capability to bind deoxyribonucleic acid (DNA). The future work of this research is based on interacting of compound with DNA and therefore the application of HE-NDI in photodynamic cancer therapy.

REFERENCES

[1] Zhan, X., Facchetti, A., Barlow, S., Marks, T. J., Ratner, M. A., Wasielewski, M. R., & Marder, S. R. (2011) Rylene And Related Diimides For Organic Electronics. *Adv. Mater*. 23: 268 – 284.

[2] Ozser, M. E., Yucekan, I., Bodapati, J.B & Icil, H. (2013) New Naphthalene Polyimide With Unusual Molar Absorption Coefficient And Excited State Properties: Synthesis, Photophysics And Electrochemistry. *J. Lumin*. 143: 542 – 550.

[3] Bodapati, J., B & Icil, H. (2011) A New Tunable Light-Emitting and Pi-Stacked Hexa-Ethyleneglycol Naphthalene-Bisimide Oligomer: Synthesis, Photophysics and Electrochemical Properties. *J. Photochem. Sci*. 10: 12831293.

[4] Asir, S., Demir, A. S., & Icil, H. (2010) The Synthesis of Novel, Unsymmetrically Substituted, Chiral Naphthalene and Perylene Diimides: Photophysical, Electrochemical, Chiroptical and Intramolecular Charge Transfer Properties. *Dyes. Pigments*. 84: 1-13.

[5] Yuney, K., & Icil, H. (2007) Synthesis, Photochemical, and Electrochemical Properties of Naphthalene- 1,4,5,8-Tetracarboxylic Acid-Bis-(N,N-bis-((2,2,4(2,2,4)-Trimethylhexylpolyimide) and Poly (N,N-bis(2,2,4(2,4,4)-trimethyl-6-aminohexyl) 3,4,9,10 Perylenetetracarboxdiimide). *Eur. Polm. J*. 43:2308-2320.

[6] Ozser, M. E., Elci, D. Uzun. I., & Icil, H. (2003) Novel Naphthalene Diimides and a Cyclophane Thereof: Synthesis, Characterization, Photophysical and Electrochemical Properties. *J. Photochem. Photobiol. Sci*. 2: 218-223.

[7] Pasaogullari, N., Demuth, M., & Icil, H. (2006) Symmetrical and Unsymmetrical Perylene Diimides: their Synthesis, Photophisical and Electrochemical Properties. *Dyes. Pigments*. 69:118-127.

[8] Uzun, D., Ozser, M. E., Yuney, K., & Icil, H. (2003) Synthesis and Photophysical Properties of N,N' – Bis-(4-Cyanophenyl) – 3,4,9,10- Perylenebis (Dicarboximide) and N,N' – Bis-(4-Cyanophenyl) – 1,4,5,8-Naphthalene Diimide. *J. Photochem. Photobiol. A: Chem*. 156:45-54.

[9] Cox, R. C., Higginbotham, H. F., Graystone, B. A., Sandanayake, S., Langford, S, J., & Bell, T. D. M. (2012) A new fluorescent H+ Sensor Based On Core-Substituted Naphthalene Diimide. *Chem. Phys. Lett*. 521: 59-63.

[10] Alp, S., Erten, S., Karapire, C., Koz, B., Doroshenko, A, O & Icli, S. (2000) Photoinduced Energy-Electron Transfer Studies With Naphthalene Diimides. *J. Photoch. Photobio A*. 135: 103-110.

[11] Heek, T., Wurthner, F., & Haag, R. (2013) Synthesis optical properties of water-soluble polyglycerol-dendronized rylene bisimide dye. *Chem. Eur*. J. 19: 10911-10921.

[12] Wurthner, F., Ahmed, S., Thalacker, C., & Debaerdemaeker, T. (2002) Core-Substituted Naphthalene Bisimides: New Flurophors With Tunable Emission Wavelenghth FRET Studies. *Chem. Eur. J*. 20: 4742-4750.

[13] Bardajee, G. R. (2013) Microwave-Assisted Solvent-Free Synthesis Of Fluorescent Naphthalimide Dyes. *Dyes. Pigments*.99:52-58.

[14] Erten, S., Posokhov, Y., Alp, S., & Icli, S. (2005) The Study Of The Solubility Of Naphthalene Diimide With Various Bulky Flanking Substituents In Different Solvents By UV-Vis Spestroscopy. *Dyes. Pigments*. 64: 171-178.

[15] Brider, T., & Gellerman, G. (2012) A Two-Step Synthesis Of Medicinally-Important 1,8Naphthalimide Peptidyls By Solid Phase Organic Synthesis. *Tetrahedron. Lett.* 53: 5611-5615.

 [16] Miller, C. T., Weragoda, R., Izbicka, E., & Iverson, B. The Synthesis And Screening Of 1,4,5,8-Naphthalenetetracarboxylic Diimide-Peptide Conjugates With Antibacterial Activity. *Bioorgan. Med. Chem*. 9: 2015-2014.

[17] Barros, T. C., Brochsztain, S., Toscano, V. G., Filho, P. B., Politi, M.J. (1997) Photophysical Characterization of a 1,4,5,8-Naphthalenediimide Derivative. *J. Photoch. Photobio. A*. 111: 97-104.

[18] Peduto, A., Pagano, B., Petronzi, C., Massa, A., Esposito, V., Virgilio, A., Massa, A., Esposito, V., Virgilio, A., Paduano, F., Trapasso, F., Fiorito, F., Florio, S., Giancola, A., & Filosa, R. (2011) Desighn, Synthesis, Biophysical And

Biological Studies Of Trisubtituted Naphthalimides As G-quadruplex Ligands. Bioorgan. *Med. Chem*. 19: 6419-6429.

[19] Barros, T. C., Brochsztain, S., Toscano, V. G., Filho, P. B., Politi, M.J. (1997) Photophysical Characterization of a 1,4,5,8-Naphthalenediimide Derivative. *J. Photoch. Photobio. A*. 111:97-104.

[20] Figueiredo, K. M., Marcon, R. O., Campos, I. B., Nantes, I. L., Brochsztain, S. (2005) Photoinduced Electron Transfer Between Cytochrome C And A Novel 1,4,5,8-Naphthalenetetracarboxylic Diimide With Amphiphilic Character. *J. Photoch. Photobio. B*. 79: 1-9

[21] Gawrys, P., Boudient, D., Malgorzata, Z., David, D., Verlhac, J. M., Horwitz, G., Pecaud, J., Pouget, S., & Pron, A. (2009) Solution Processible Naphthalene And Prylene Bisimides: Synthesis, Electrochemical Characterization And Application To Organic Field Effect Transistor (OFETs) Fabrication. Synthetic. Met. 159: 1478-1485.

[22] Wang, J., C. (1980) Superhelical DNA. Trends. Biochem. Sci. 5: 219-221.

[23] Watson, J. D., & Crick, F. H. C. (1953) The structure of DNA.Cold. Spring. *Harb. Sym*. 18:123-131.

[24] Crick, F, H, C., & Watson, J, D. (1954) The Complementary Structure of Deoxyribonucleic Acid. *Proc. R. Soc. Lond. A*. 223: 80-96.

[25] Bidzinska, J., Cimino-Reale, G., Zaffarono, N., & Folini, M. (2013) G-Quadruplex Structures in the Human Genomes as Novel Therapeutic Targets. *Molecules*. 18: 12368-12395.

[26] Yaku, H., Murashima, T., Miyoshi, D., & Sugimoto, N. (2012) Specific Binding of Anionic Porphyrin and Phthalocyanine to the G-quadruplex with a Variety of in Vivo Application.*Molecules*. 17: 10586-10613.

[27] Bronowska, A. K. (2006) Thermodynamics of Ligand-Protein Interactions:Implications for Molecular Design. *Chem. Int. Ed. Engl*. 35: 2588-2614.

[28] Stevens, A. L., Janssen, P. G. A., Ruiz-Carretero, A., Surin, M., Schenning, A. P. H. J., & Herz, L. M., (2011) Energy Transfer in Single-Strand DNA-Template Stacks of Naphthalene Chromophores. *J. Phys. Chem.* 115: 1055-10560.

[29] Hai-jun, N., Jing-Shan, M., Mi-lin, Z., Jun, L., Pei-Hui, L., Xu-Duo., & Wen, W. (2009)Naphthalene-Containing Polyimides:Synthesis, Characterization and Photovoltaic Properties of Novel Doner-Acceptor Dyes Used in Solar Cell. Trans. *Noferrous Met. Soc. China.* 19: 587-593.

[30] Yiseen, A. G. (2014) Synthesis and Characterization of new Monomer and new Polymer of Naphthalene diimid:Electrochemical and Optical Studies. *Int. J. Electrochem. Sci*. 9: 2575-2588.

[31] Gong, J., Liang, J., & Sumathy, K. (2012) Review on Dye-sensitized Solar Cells (DSSC$_S$): Fundamental concepts and novel materials. Renew. *Sust. Energ. Rev*. 16: 5848-5860.

[32] Cravino, A., Schilinsky, P., & Brabec, J. B. (2007) Characterization of Organic Solar Cells: the Importance o Device Layout. *Adv. Funkt. Mater*. 17: 3906-3910.

[33] Turro, N.J. (1965) Molecular Photochemistry, Benjamin, London, 44.